

# glyndŵr

PRIFYSGOL GLYNDŴR WRECSAM  
GLYNDŴR UNIVERSITY WREXHAM

Subject Area of  
**Aeronautical-Mechanical Engineering**

**B.Eng (Hons) Aeronautical & Mechanical Engineering**

**Final Year Project Report**

***CFD ANALYSIS OF WINGLETS***

Name: Amador Calvo Portillo

Supervisor: Md. Salim Miah

Date: May 2011

## ABSTRACT

The purpose of this project is to analyse different types of winglets using Gambit and Fluent and then, to find out what happens when winglets are linked to wingtips. One wing model without winglet and three wing models with winglets were created and drawn in Solid Edge and they were meshed in Gambit using geometry data gathered by the Airfoil Investigation Database and Airbus website. Those models were read into Fluent where flow boundary conditions were applied and the discretized Navier-Stokes equations were solved numerically.

The wing without winglet and the wings with winglets performance were analyzed in several angles of attack and the drag coefficient was compared when the aircraft is taking off. Wingtip vortices from models were checked, studied and compared. The best winglet model reduces drag coefficient and wingtip vortices from wing without winglet model and it will be pointed out at the end of this project. There was a test in order to analyse the models when the aircraft works in cruise velocity. Unfortunately, as I was running out of time, this task was not successfully completed.

## ACKNOWLEDGEMENTS

I would like to thank my supervisor Md. Salim Miah for his help and support without which this project would never have been completed. Also, my father and my grandparents rest in peace, my mother, my brother and my sister who have always supported me in everything.

## TABLE OF CONTENTS

<b>1 INTRODUCTION</b>	1
<b>2 AIMS OF PROJECT</b>	2
<b>3 REVIEW OF LITERATURE</b>	3
<u>3.1 Mach number</u>	3
<u>3.2 Viscosity</u>	4
<u>3.3 Reynolds number</u>	4
<u>3.4 Aerodynamic forces</u>	5
<u>3.5 Lift and drag</u>	6
<u>3.6 Bernoulli's principle</u>	8
<u>3.7 Continuity equation</u>	8
<u>3.8 Wingtip vortex development</u>	9
<u>3.9 Winglets</u>	12
<u>3.10 Types of winglets</u>	14
<b>3.10.1 Wingtip fence</b>	14
<b>3.10.2 Blended winglets</b>	14
<b>3.10.3 Raked wingtips</b>	15
<u>3.11 Computational Fluids Dynamics (CFD)</u>	17
<b>4 EXPERIMENTAL PROCEDURES</b>	20
<u>4.1 Solid Edge v18</u>	20
<u>4.2 Gambit 2.4.6</u>	25
<u>4.3 Fluent 6.3.26</u>	28
<b>5 RESULTS AND DISCUSSION</b>	30
<u>5.1 CFD Analysis of wingtip vortices development</u>	30
<u>5.2 CFD Analysis of wingtip vortices performance</u>	35
<b>5.2.1 Vortex rotation</b>	36
<b>5.2.2 Wingtip vortex motion</b>	37
<u>5.3 Winglets performance</u>	46
<b>5.3.1 Winglets performance at 4°</b>	46
<b>5.3.2 Winglets performance at 8°</b>	48
<b>5.3.3 Winglets performance at 12°</b>	50
<u>5.4 Wingtip vortex reduction</u>	52

<u>5.5 Drag coefficient improvement</u>	53
<b>6 CONCLUSIONS</b>	55

<b>7 RECOMMENDATIONS</b>	56
<b>8 REFERENCES</b>	57
<b>9 APPENDIX A</b>	59

## TABLE OF FIGURES

Fig.1: <i>four forces of flight.</i>	5
Fig.2: <i>airfoil lift and drag due to lift.</i>	5
Fig.3: <i>pressure in an airfoil.</i>	6
Fig.4: <i>wingtip vortex development I.</i>	9
Fig.5: <i>wingtip vortex development II.</i>	10
Fig.6: <i>winglets on a Virgin Atlantic Airbus A340-600.</i>	12
Fig.7: <i>wingtip vortex with and without winglet.</i>	13
Fig.8: <i>Peugeot 908 HDI-winglets double.</i>	13
Fig.9: <i>Airbus Winglets as seen from the outsider.</i>	14
Fig.10: <i>Airbus Winglets as seen from onboard.</i>	14
Fig.11: <i>blended winglets.</i>	15
Fig.12: <i>raked wingtips on the new Boeing 787 and Airbus A350.</i>	16
Fig.13: <i>types of winglets.</i>	16
Fig.14: <i>A330-300 general dimensions.</i>	20
Fig.15: <i>naca 2415 airfoil.</i>	21
Fig.16: <i>naca 2415 airfoil in Solid Edge v18.</i>	21
Fig.17: <i>wing model construction.</i>	21
Fig.18: <i>wing model completed.</i>	22
Fig.19: <i>wing model with blended winglet completed.</i>	22
Fig.20: <i>blended winglet model zoom.</i>	23
Fig.21: <i>wingtip fence model completed and plans.</i>	23
Fig.22: <i>circular profiles and wing model completed.</i>	24
Fig.23: <i>circular winglet model zoom.</i>	24
Fig.24: <i>control zones and wind tunnel circular winglet 12°.</i>	25
Fig.25: <i>mesh circular winglet 12°. Interval size 1,5.</i>	26
Fig.26: <i>wing mesh. Interval size &lt; 0.1 depending on winglet.</i>	26
Fig.27: <i>control zones mesh. Interval size 0,3.</i>	27
Fig.28: <i>volume control zones mesh. Interval size 0,5.</i>	27
Fig.29: <i>control zones blended winglet 8°. Isometric view.</i>	
<i>Orthographic projection.</i>	28
Fig.30: <i>control zones blended winglet 8°. Back view.</i>	





Fig.31: <i>grid blended winglet 8°.</i>	29
Fig.32: <i>grid blended winglet 8° II.</i>	29
Fig.33: <i>contours of vorticity magnitude (1/s) at 0° in control zones. No winglet.</i>	31
Fig.34: <i>contours of vorticity magnitude (1/s) at 4° in control zones. No winglet. Orthographic projection.</i>	31
Fig.35: <i>surface at wingtip to work out pressure difference. Perspective projection.</i>	32
Fig.36: <i>contours of total pressure (Pa) 0° no winglet at wingtip.</i>	33
Fig.37: <i>contours of total pressure (Pa) 4° no winglet at wingtip.</i>	33
Fig.38: <i>contours of total pressure (Pa) 8° no winglet at wingtip.</i>	33
Fig.39: <i>contours of total pressure (Pa) 12° no winglet at wingtip.</i>	34
Fig.40: <i>contours of total pressure (Pa) 16° no winglet at wingtip.</i>	34
Fig.41: <i>wingtip vortex performance.</i>	35
Fig.42: <i>contours of X-vorticity (1/s) iso-clip surface. Circular winglet 8°. Orthographic projection.</i>	36
Fig.43: <i>contours of X-vorticity (1/s). Circular winglet 8°. Orthographic projection.</i>	37
Fig.44: <i>reference system. Orthographic projection.</i>	38
Fig.45: <i>reference system. Front view. Orthographic projection.</i>	38
Fig.46: <i>contours of vorticity magnitude (1/s) blended winglet at 4°. Orthographic projection.</i>	39
Fig.47: <i>contours of vorticity magnitude 4°. No winglet. Orthographic projection.</i>	46
Fig.48: <i>contours of vorticity magnitude 4°. Circular winglet. Orthographic projection.</i>	46
Fig.49: <i>contours of vorticity magnitude 4°. Wingtip fences. Orthographic projection.</i>	47
Fig.50: <i>contours of vorticity magnitude (1/s) blended winglets. Orthographic projection.</i>	
Fig.51: <i>contours of vorticity magnitude (1/s) no winglet. Orthographic projection.</i>	

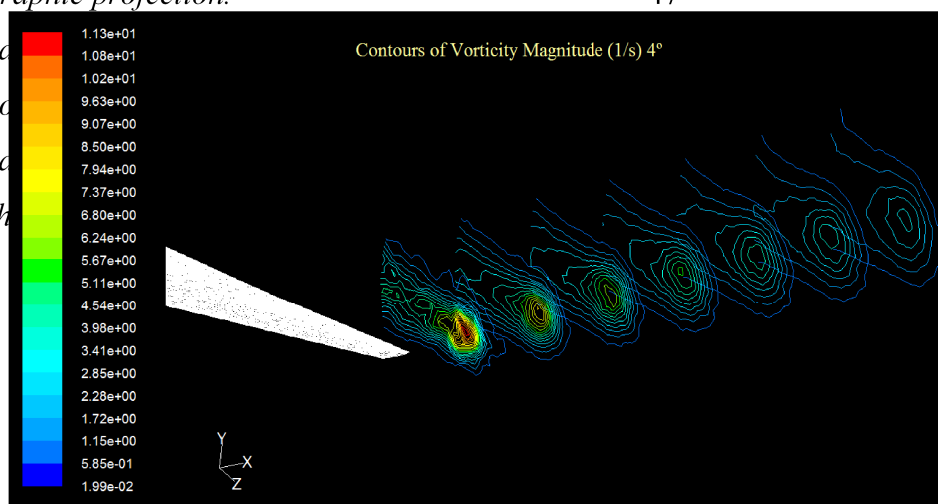


Fig.52: *contours of vorticity magnitude  $8^\circ$ .*

*Circular winglet. Orthographic projection.*

48

Fig.53: <i>contours of vorticity magnitude 8°. Wingtip fence.</i> <i>Orthographic projection.</i>	49
Fig.54: <i>contours of vorticity magnitude 8°. Blended winglet.</i> <i>Orthographic projection.</i>	49
Fig. 55: <i>contours of vorticity magnitude 12°. No winglet.</i> <i>Orthographic projection.</i>	50
Fig.56: <i>contours of vorticity magnitude 12°. Circular winglet.</i> <i>Orthographic projection.</i>	50
Fig.57: <i>contours of vorticity magnitude 12°. Wingtip fence.</i> <i>Orthographic projection.</i>	50
Fig.58: <i>contours of vorticity magnitude 8°.Blended winglet.</i> <i>Orthographic projection.</i>	51
Fig. 59: <i>wingtip vortex reduction.</i>	52

## TABLE OF GRAPHICS

Graphic.1: <i>X-Vorticity vs. X-coordinate .Circular winglet 8°.</i>	36
Graphic.2: <i>vorticity magnitude vs. Y-coordinate. (transform-30). Blended winglet at 4°.</i>	39
Graphic.3: <i>vorticity magnitude vs. Y-coordinate. Control zone-1. Blended winglet at 4°.</i>	40
Graphic.4: <i>vorticity magnitude vs. Y-coordinate. Control zones-2 and 3. Blended winglet at 4°.</i>	40
Graphic.5: <i>vorticity magnitude vs. Y-coordinate. Control zones-4 and 5. Blended winglet at 4°.</i>	40
Graphic.6: <i>vorticity magnitude vs. Y-coordinate. Control zone-6. Blended winglet at 4°.</i>	41
Graphic.7: <i>vorticity magnitude vs. Y-coordinate. Control zone-7. Blended winglet at 4°.</i>	41
Graphic.8: <i>vorticity magnitude vs. X-coordinate. All zones. Blended winglet at 4°.</i>	41
Graphic.9: <i>Y-coordinate vs. Distance at wingtip.</i>	42
Graphic.10: <i>vorticity magnitude vs. Z-coordinate. (transform-30). Blended winglet at 4°.</i>	43
Graphic.11: <i>vorticity magnitude vs. Z-coordinate. Control zone-1. Blended winglet at 4°.</i>	43
Graphic.12: <i>vorticity magnitude vs. Z-coordinate. Control zone-2. Blended winglet at 4°.</i>	43
Graphic.13: <i>vorticity magnitude vs. Z-coordinate. Control zone-3. Blended winglet at 4°.</i>	44
Graphic.14: <i>vorticity magnitude vs. Z-coordinate. Control zone-4. Blended winglet at 4°.</i>	44
Graphic.15: <i>vorticity magnitude vs. Z-coordinate. Control zone-5. Blended winglet at 4°.</i>	44
Graphic.16: <i>vorticity magnitude vs. Z-coordinate. Control zone-6. Blended winglet at 4°.</i>	45
Graphic.17: <i>vorticity magnitude vs. Z-coordinate. Control zone-7.</i>	

*Blended winglet at 4°.*

45

## TABLES

Table.1: <i>wing areas.</i>	24
Table.2: <i>total sum of vorticity magnitude (1/s) at 4° in control zones.</i>	48
Table.3: <i>total sum of vorticity magnitude (1/s) at 8° in control zones.</i>	49
Table.4: <i>total sum of vorticity magnitude (1/s) at 12° in control zones.</i>	51
Table.5: <i>aerodynamic coefficients. Without winglet.</i>	53
Table.6: <i>aerodynamic coefficients. Circular winglet.</i>	53
Table.7: <i>aerodynamic coefficients. Wingtip fence.</i>	53
Table.8: <i>aerodynamic coefficients. Blended winglet.</i>	53
Table.9: <i>drag coefficient improvement.</i>	54

## TABLE OF EQUATIONS

[3.1] <i>Mach number</i>	3
[3.2] <i>Reynolds number</i>	4
[3.3] <i>Lift</i>	6
[3.4] <i>Drag</i>	7
[3.5] <i>Bernoulli equation</i>	8
[3.6] <i>Continuity equation</i>	8
[3.7] <i>Continuity equation</i>	8
[3.8] <i>Induced drag</i>	11
[3.9] <i>Induced drag coefficient</i>	11
[3.10] <i>Aspect ratio</i>	11
[3.11] <i>Drag coefficient</i>	11
[3.12] <i>Equation of momentum</i>	17
[3.13] <i>Equation of energy conservation</i>	17





## 1 INTRODUCTION

Since the 1970s, when the price of aviation fuel began spiralling upward, airlines and aircraft manufactures have looked at many ways to improve the operating efficiency of their aircraft. Winglets have become one of the industry's most visible fuel saving technologies and their use continues to expand. Moreover, they can reduce fuel consumption about 4% in many flights when the distance to crossing is more than 1800 km. Winglets are vertical extensions of wingtips that improve an aircraft's fuel efficiency and cruising range. Designed as small airfoils, they reduced the aerodynamic drag associated with vortices that develop at the wingtips. If aircraft's fuel efficiency goes down means drag coefficient is reduced (Marty Curry, 2008). Drag coefficient reduction will be checked and compared when winglets are used. For that, three wings models with different types of winglets will be analyzed in different angles of attack. Besides, a wing model without winglet will be studied and the results can be compared. The wing was made of a naca 2415 airfoil. The drag coefficient reduction has similarities to wingtip vortex which is developed when the aircraft moves through the air. Therefore, wingtip vortex will be analyzed and we may check how the vorticity magnitude can be reduced with winglets.

A-330 wing was built and the winglets were fixed at the wingtip. The wing was created and drawn in Solid edge v18 and it was imported to Gambit 2.4.6 to mesh the different models. I would say mesh models is one of the worst and difficult task in my project, indeed. The different types of wings with winglets and without winglet were analyzed and compared in Fluent 6.3.26. Several tables, diagrams or figures will be used to show the vorticity magnitude, the wingtip vortices and the drag coefficient reduction.

Blended winglet, wingtip fence and circular winglet have been used to demonstrate wingtip vortex and drag coefficient go down when they are used in the aircrafts. Airfoil 0012 was used to create blended winglet and wingtip fence. That is a symmetrical airfoil so it must be used in my models since it is not able to develop a high lift coefficient which would make it wrong to winglet performance. Finally, a winglet will be chosen due to drag coefficient's reduction when that winglet will be working at the wingtip. Furthermore, as this winglet has been previously picked, I will make a point linked to it, and the drag coefficient reduction will be showed in a final table.

## **2 AIMS OF PROJECT**

At the beginning of this remarkable project, my knowledge and skills in Gambit and Fluent were not very deep and wide. I decided to do this project in order to improve my Gambit and Fluent skills. Gambit and Fluent are one of the most popular software among aeronautical industry, therefore I realised I should be in more touch with it. I am not an expert Gambit and Fluent user, however after working with this software during the last months I am positive my Gambit and Fluent skills have been improved (as a matter of a fact, I have successfully completed this project) and one of my proposed objectives has been reached.

On the other hand, when the aircraft moves through the air, it results into the production of wingtip vortices due to its own lifting. These wingtip vortices are higher as the aircraft lift increases. If winglets are fixed to wingtips, then such wingtip vortex goes down and the aircraft performance will turn out to be better. I have hardly emphasized on the analyses and wingtip vortex development and performance.

When winglets are used, drag coefficient decreases since wingtip vortices are broken or reduced by winglets. The drag coefficient reduction and why it is reduced will be the main aim to study and develop in my project.

Finally, I would like to demonstrate and prove winglet works more efficiently and, in addition, to show how drag coefficient can be reduced. That is the main reason why aircraft's fuel efficiency can be improved if winglets are linked to wingtips.

### 3 REVIEW OF LITERATURE

In this project, Computational Fluids Mechanist analysis of winglets have been done therefore it is absolutely necessary to understand the aerodynamics concepts.

Aerodynamics from the union of two Greek words: eros, which means air, and dynamis, meaning power. Thus, aerodynamics is the study of forces and movements that occur in objects through the air. A more current definition of the term aerodynamics: the branch of fluid mechanics that studies the actions on the solid objects when there is relative motion between them and the fluid that bathes them.

There are different classifications for aerodynamic problems. First classification is made depending on the nature of the fluid:

-Incompressible flow, when the air velocity,  $v$ , is lower than  $0.3 \times M$  ( $M$ = Mach number,  $M=1$  if  $v=340$  m/s).

-Compressible flow, the air velocity,  $v$ , is higher than  $0.3 \times M$ .

Second classification is made depending on Mach number:

-Subsonic, flow velocity is always lower than sound velocity,  $M < 1$ . All commercial aircraft are flying below  $M=1$ .

-Transonic, flow velocity is close to  $M=1$ .

-Supersonic, flow velocity is higher than  $M=1$  in all areas of the wing.

-Hypersonic, when the flow velocity is much higher than sound velocity, about  $M > 6$ .

#### 3.1 Mach number

The Mach number is a number that is used as speed reference. The Mach number is used to assess whether the phenomena due to the change in air density-compressibility- have or not very important, that is to say, if they are negligible.

We define the Mach number as shown in equation [3.1] and we see that when the fluid velocity is equal to the speed of sound we have  $M = 1$ .

$$M = \frac{V}{C} = \frac{\text{speedflow}}{\text{speedsound}} \quad [3.1]$$

### 3.2 Viscosity

Viscosity is a measure of the resistance of a fluid which is being deformed by either shear stress or extensional stress. In other words, Viscosity is a measure of a fluid's resistance to flow. It describes the internal friction of a moving fluid. A fluid with large viscosity resists motion because its molecular make up gives it a lot of internal friction. In general, in any flow, layers move at different velocities and the fluid's viscosity arises from the shear stress between the layers that ultimately oppose any applied force.

Isaac Newton postulated that, for straight, parallel and uniform flow, the shear stress,  $\tau$ , between layers is proportional to the velocity gradient  $\partial u / \partial y$ , in the direction perpendicular to the layers (M.A. Soliman, 2009).

In fact, due to the air is a viscous fluid airplanes can fly. If the air had no viscosity, the fluid layers not travel attached to the wing surface, and not show the forces that allow the flight.

### 3.3 Reynolds number

The Reynolds number relates the density, viscosity, speed and size of a typical flow in a dimension less expression, which is involved in many fluid dynamics problems. This dimensionless number or combination appears in many cases related to the fact that laminar flow can be seen (small Reynolds number) or turbulent (Reynolds number largest). From a mathematical point of view the Reynolds number of a problem or situation is defined by the following equation:

$$\text{Re} = \frac{\rho V L}{\mu} = \frac{V L}{\nu} = \frac{Q L}{\nu A} \quad [3.2]$$

where:

$V$  is the mean fluid velocity (m/s)

$L$  is a characteristic linear dimension (m)

$\mu$  is the dynamic viscosity of the fluid (Pa·s or N·s/m<sup>2</sup> or kg/(m·s))

$\nu$  is the kinematic viscosity ( $\nu = \mu / \rho$ ) ( $\text{m}^2/\text{s}$ )

$\rho$  is the density of the fluid ( $\text{kg}/\text{m}^3$ )

### 3.4 Aerodynamic forces

Aerodynamic forces are those displayed by the fact of having a body moves at speed immersed in a fluid. There are the following forces in an aircraft:

-Weight, although not strictly an aerodynamic force is always present, and will determine the lift we need to keep the plane in the air. It is a force that is always directed toward the centre of the earth. The magnitude of the weight depends on the mass of all the airplane parts, plus the amount of fuel, plus any payload on board (people, baggage, freight, etc.) (Tom Bensom, 2010).

-Lift, the lift is the force perpendicular to the direction of the freestream. To overcome the weight force, airplanes generate an opposing force called lift. The magnitude of the lift depends on several factors including the shape, size, and velocity of aircraft.

-Drag, the drag is defined as the force component in the direction of the freestream. As the airplane moves through the air, there is another aerodynamic force present. The air resists the motion of the aircraft and the resistance force is called drag. Like lift, there are many factors that affect the magnitude of the drag force (Tom Bensom, 2010).

-Thrust, is not an aerodynamic force. To overcome drag, airplanes use a propulsion system to generate a force called thrust.

The figure 1, reproduced below, shows the forces in an aircraft.

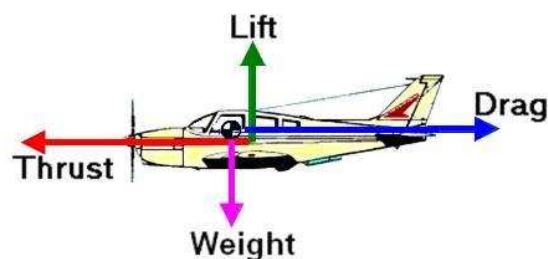


**Fig.1: four forces of flight.**

The figure 2, reproduced below, shows the drag and lift force in an airfoil.

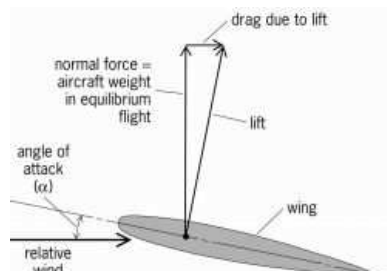


**Fig.2: airfoil lift and drag due to lift.**

### 3.5 Lift and drag

When there is a fluid moves through the wing, forcing air particles to narrow at the upper surface of the wing, while the air particles that travel at the lower surface of the wing are expanded. That effect can be seen from Figure 3.

Therefore, the flow velocity is increased at the upper surface and the pressure goes down. On the other hand, the flow velocity drops at the lower surface and the pressure grows. The pressure difference between lower and upper surface generates an aerodynamic force called lift. In the figure 3, the pressures caused can be seen in red colour.

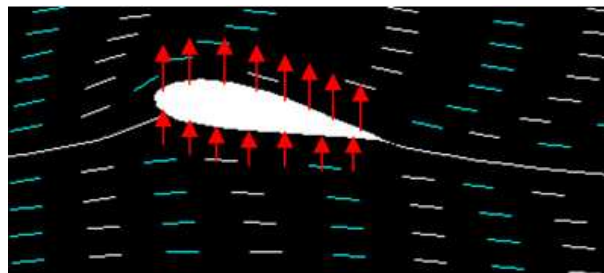


**Fig.3: pressure in an airfoil.**

When a stream of air moves over a profile produces a force called aerodynamics. This force is usually decomposed into two components: Lift and Drag. The lift,  $L$ , is the component perpendicular to the free flow of air, and  $L$  is defined by the following the equation:

$$L = \frac{1}{2} \times \rho \times V^2 \times S \times Cl \quad [3.3]$$

where:

$\rho$  is the density of the fluid through which the body is moving.

$V$  is the speed of the body relative to the fluid.

$S$  is the reference area or wing area.

$Cl$  is the lift coefficient.

With the equation [3.3] is really easy to work out the lift coefficient. The lift coefficient (Tom Bensom, 2009) is a number that aerodynamicists use to model all of the complex dependencies of [shape](#), inclination, and [some flow conditions](#) on lift. This equation is simply a rearrangement of the [lift equation](#) where we solve for the lift coefficient in terms of the other variables. The lift coefficient  $Cl$  is equal to the lift  $L$  divided by the quantity: density  $\rho$  times half the velocity  $V$  squared times the wing area  $S$ .

The drag force is the resistance force caused by the motion of a body through a fluid, such as water or air. A drag force acts opposite to the direction of the oncoming flow velocity. This is the relative velocity between the body and the fluid.

The drag force  $D$  exerted on a body travelling through a fluid is given by:

$$D = \frac{1}{2} \times \rho \times V^2 \times S \times Cd \quad [3.4]$$

where:

$\rho$  is the density of the fluid through which the body is moving.

$V$  is the speed of the body relative to the fluid.

$S$  is the projected cross-sectional area of the body perpendicular to the flow direction

$Cd$  is the drag coefficient.

The drag coefficient can be computed from equation [3.4]. The drag coefficient is a measure adimensional that describes the amount of aerodynamic drag caused by fluid flow, used in the drag equation. Two objects of the same frontal area moving at the same speed through a fluid experience a drag proportional to its  $Cd$ .

In general,  $Cd$  is not an absolute constant for a given body shape. It varies with the speed of airflow (or more generally with Reynolds number). A smooth sphere, for example, has a  $Cd$  that varies from high values for laminar flow to 0.47 for turbulent flow. A dimensionless number used in aerodynamics to describe the drag of a shape.

The drag coefficient,  $Cd$ , is independent of the size of the object and is usually determined in a wind tunnel.

The lift generates by an airfoil, and by extension, the wings will depend on the altitude and speed aircraft, and the lift coefficient which has our airfoil. There are two different ways to increase the lift: increasing the angle of attack or speed.

Increase the angle of attack causes an increase in the  $Cl$ , but this has a limit, as speed

increases, and that from a certain angle, or velocity, the air starts to come off the wing. When the air begins to travel not attached to the wing, it generates lift. This effect usually begins at the trailing edge in the airfoils furthest from the fuselage of the plane, and extends to the edge and the centre of the plane. To explain why these aerodynamic forces are produced we must use two physical principles: Bernoulli's principle and continuity equation.

### 3.6 Bernoulli's principle

Bernoulli's Principle, also known as the triad of Bernoulli or Bernoulli's equation describes the behaviour of a fluid moving along a streamline. It states that an ideal fluid without viscosity or friction, running through a closed pipeline, total energy remains constant throughout its length. This means an increase in flow speed lead to a reduction of pressure, and conversely, if the flow speed is reduced the pressure increases. The Bernoulli equation is given by:

$$\frac{V^2 \times \rho}{2} + p + \rho \times g \times z = \text{const} \quad [3.5]$$

### 3.7 Continuity equation

In [fluid dynamics](#), the continuity equation is a mathematical statement that, in any [steady state](#) process, the rate at which mass enters a system is equal to the rate at which mass leaves the system. The differential form of the continuity equation is:

$$\frac{\partial \rho}{\partial t} + \nabla \cdot (\rho u) = 0 \quad [3.6]$$

where  $\rho$  is fluid [density](#),  $t$  is time, and  $u$  is the [flow velocity vector field](#). If density ( $\rho$ ) is a constant, as in the case of [incompressible flow](#), the mass continuity equation simplifies to a volume continuity equation:

$$\nabla \cdot u = 0 \quad [3.7]$$

Concepts basics of aerodynamics have been explained until now. From now, wingtip vortex development, winglets effects and winglets technology will be discussed.



### 3.8 Wingtip vortex development

Vortices form because of (U.S Centennial of Flight Commission, n.d) the difference in pressure between the upper and lower surfaces of a wing that is operating at a positive lift. Since pressure is a continuous function, the pressures must become equal at the wing tips. The tendency is for particles of air to move from the lower wing surface around the wing tip to the upper surface (from the region of high pressure to the region of low pressure) so that the pressure becomes equal above and below the wing. In addition, there exists the oncoming free-stream flow of air approaching the wing. If these two movements of air are combined, there is an inclined inward flow of air on the upper wing surface and an inclined outward flow of air on the lower wing surface. The flow is strongest at the wing tips and decreases to zero at the midspan point as evidenced by the flow direction there being parallel to the free-stream direction.

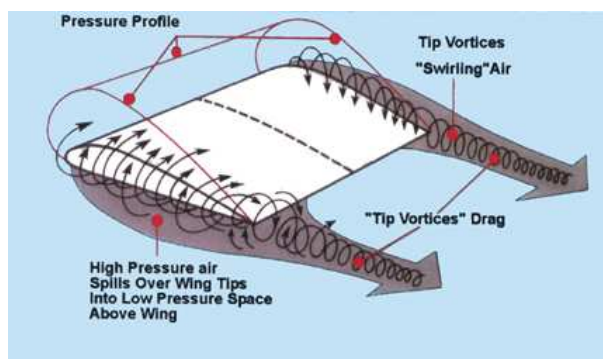


**Fig.4: wingtip vortex development I**

When the air leaves the trailing edge of the wing, the air from the upper surface is inclined to that from the lower surface, and helical paths, or vortices, result. A whole line of vortices trails back from the wing, the vortex being strongest at the tips and decreasing rapidly to zero at midspan. A short distance downstream, the vortices roll up and combine into two distinct cylindrical vortices that constitute the wingtip vortices. The wingtip vortices trail back from the wing tips and they have a tendency to sink and roll toward each other downstream of the wing. Again, eventually the tip vortices dissipate, their energy being transformed by viscosity.

The tip vortices cause additional downflow (or downwash) behind the wing within the wingspan. For an observer fixed in the air, all the air within the vortex system is moving downward (called downwash) whereas all the air outside the vortex system is moving upward (called upwash). An aircraft flying perpendicular to the flight path of the airplane creating the vortex pattern will encounter upwash, downwash, and upwash in that order. The gradient, or change of downwash to upwash, can become very large at the tip vortices and cause extreme motions in the airplane flying through it. An airplane flying into a tip vortex also has a large tendency to roll over. If the [control surfaces](#) of the airplane are not effective enough to counteract the airplane roll tendency, the pilot may lose control or, in a violent case, experience structural failure.

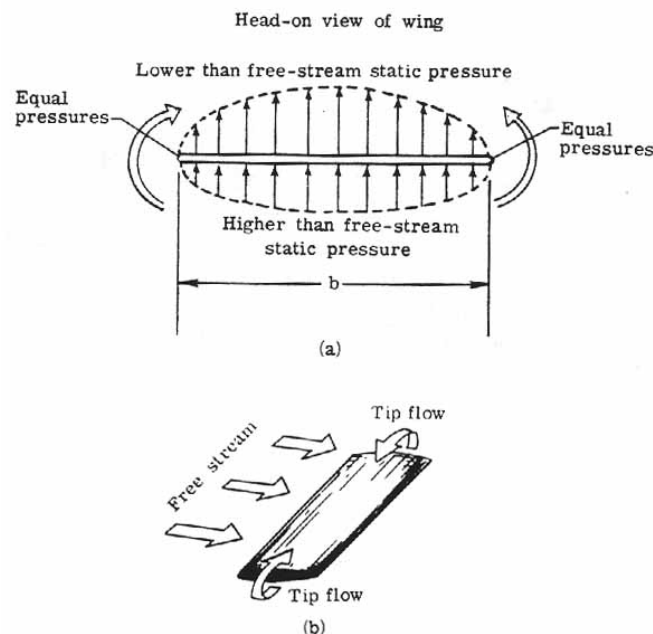


**Fig. 5: wingtip vortex development II**

Pressures must become equal at the wing tips since pressure is a continuous function (figure 5 a). The free stream flow combines with tip flow, resulting in an inward flow of air on the upper wing surface and an outward flow of air on the lower wing surface (figure 5 b).

These vortices are a problem on several levels. For the plane itself, increase the induced drag: you have to waste energy on accelerating the mass of air rather than use it in their own advancement. And for rest of aircraft, such turbulence remain airborne for several minutes (down slowly to about 100 m/min and laterally away about 5 km/h). Worst of all is that these wingtip vortices are strongest at low speeds (landing and takeoff), being able to pull an airplane.

The effect of the presence of these vortices is the creation of a stream of air downward, after the wing, called downwash, or induced velocity ( $w_i$ ), which is directly responsible for the appearance of one of the components of resistance aerodynamic, induced drag ( $D_i$ ). This resistance is inextricably linked to the lift. The equation [1.8] shows induced drag.

$$D_i = \frac{2L^2}{\rho \pi b^2 V^2 e} \quad [3.8]$$

where:

L is the lift,  $\rho$  fluid density, b is wingspan, V velocity and e is efficiency factor, in general  $e < 1$  and depends on the wing shape.

The induced drag coefficient showed in equation [3.9],  $C_{di}$  is equal to the square of the lift coefficient  $C_l$  divided by the quantity:  $\pi$  (3.14159) times an efficiency factor times the aspect ratio AR.

$$C_{di} = \frac{C_l^2}{\pi e AR} \quad [3.9]$$

The [aspect ratio](#) is the square of the span s divided by the wing area A.

$$AR = \frac{s^2}{A} \quad [3.10]$$

It is also called "drag due to lift" because it only occurs on finite, lifting wings and the magnitude of the drag depends on the lift of the wing. Induced drag is (Tom Bensom, 2010) a three dimensional effect related to the wing tips; induced drag is a wing tip effect. So if the wing tip represents only a [small fraction](#) of the total wing area, the

induced drag will be small. Again, long thin wings have low induced drag. For many years, wing designers have attempted to reduce the induced drag component by special shaping of the wing tips. The Wright Brothers used curved trailing edges on their rectangular wings based on [wind tunnel results](#). The outstanding aerodynamic performance of the British Spitfire of World War II is partially attributable to its elliptic shaped wing which gave the aircraft a very low amount of induced drag. On modern airliners, the wing tips are often bent up to form [winglets](#). Winglets were invented by Richard Whitcomb of the NASA Langley Research Center in an effort to reduce the induced drag on airliners.

For a wing, the total [drag coefficient,  \$C\_d\$](#)  is equal to the base drag coefficient at zero lift  $C_{d0}$  plus the induced drag coefficient  $C_{di}$ .

$$C_d = C_{d0} + C_{di} \quad [3.11]$$

### 3.9 Winglets

Many of us (Airline world, n.d) who fly regularly have most probably seen a so-called winglet or wingtip device at the end of the wing of an airliner at least once. It is showing up more and more often on more and more types of aircraft, thus we felt it's time to give an overview to our readers about these sometimes funny, sometimes cool and stylish looking aircraft parts.



**Fig.6: Winglets on a Virgin Atlantic Airbus A340-600.**

The initial theoretical concept goes back to times before even the Wright Brothers first took to the skies in 1905, but it was picked up and developed by Richard T. Whitcomb of NASA after the 1973 oil crisis – in order to reduce fuel consumption. The first tests were carried out in 1979/80 in cooperation with the U.S. Air Force. At almost the same time, but independent of any U.S. military organization, a private jet producer, Lear Jet exhibited a prototype in 1977: the Lear Jet 28 that featured the first winglets on a jet and a production aircraft. Flight tests made with and without winglets showed that the winglets increased range by about 6.5 percent and also improved directional stability for the Lear Jet- these two factors are the major reasons behind using this facility at any fixed wing aircraft ever since.

A winglet is a (near) vertical extension of the wing tips. Designed as small airfoils, winglets reduced the aerodynamic drag associated with vortices that develop at the wingtips as the airplane moves through the air. By reducing wingtip drag, fuel consumption goes down and range is extended. Aircraft of all types and sizes are flying with winglets. From single-seat hang gliders and ultralights to global jumbo jets. Some aircraft are designed and manufactured with sleek upturned winglets that blend smoothly into the outer wing sections. The upward angle of the winglet, its inward angle as well as its size and shape are critical for correct performance – this is why they can look quite different. Air rotating around the wing strikes the surface of the winglet that directs it in another direction – thus creating an extra force, basically converting otherwise wasted energy to thrust. This is a small contribution but can save a lot for an operator in an aircraft's lifetime. Another potential benefit of winglets is that they reduce the strength of wingtip vortices, which trail behind the plane. When other aircraft pass through these vortices, the turbulent air can cause loss of control, possibly resulting in an accident (Airline world, n.d).

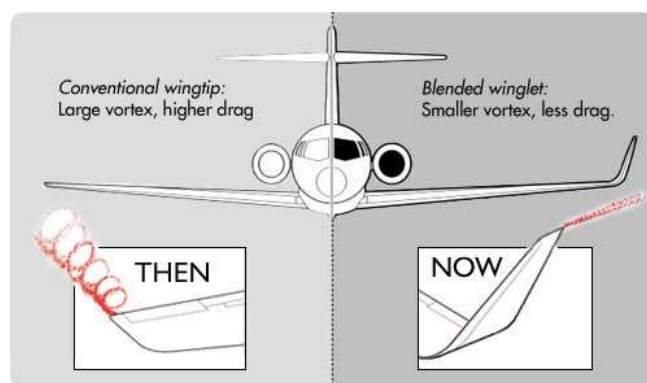


**Fig.7: wingtip vortex with and without winglet.**

Since the 1970s, when the price of aviation fuel began spiralling upward, airlines and aircraft manufactures have looked at many ways to improve the operating efficiency of their aircraft. Winglets have become one of the industry's most visible fuel saving technologies and their use continues to expand.

Their main functions are: improved wing efficiency translates to more payload, reduced fuel consumption (about 4% in many flights when the distance to crossing is more than 1800 Km.), and a longer cruising range that can allow an air carrier to expand routes and destinations.

With winglets aerodynamic drag goes down, so these components are often used in car industry. Winglets are used in cars of high range or even in formula 1.



**Fig.8: Peugeot 908 HDI-winglets double.**

### 3.10 Types of winglets

In general any wingtips (Airline world, n.d) that not end the wing simply horizontally are considered as some kind of a winglet. Even though in strictly technical terms Wingtip Fences are not real extensions of the wing, and Raked Wingtips do not have a vertical part, they are still widely considered as winglet variants. We can distinguish three types of winglets: wingtip fences, blended winglets and raked wingtips. The different types of winglets are explained showing various images and commenting on the aircraft in which they are used.

#### **3.10.1 Wingtip fence**

They are a special variant of winglets that extend both upward and downward from the tip of the wing. Preferred by European plane-maker Airbus, it is featured on their full

product range (except the A330/340 family and the future A350). The Airbus A300 was actually the first jet airliner to feature this kind of solution by default, but it was a very small version of the tool. Provided that most of the Airbus planes (including all A320 family jets) feature such wingtip fences, this may be the most seen and most produced winglet type. Even the new Airbus A380 double-decker features wingtip fences.



**Fig.9: Airbus Winglets as seen from the outsider.**



**Fig.10: Airbus Winglets as seen from onboard.**

### 3.10.2 Blended winglets

They know as the real “Winglets”. They are the most popular winglet type, leveraged by Airbus, Boeing, Embraer and Bombardier but also by Russian Tupolev and Iljushin. Blended winglets were first introduced on the McDonnell Douglas MD-11 aircraft in 1990 with launch customer Finnair (it also features a smaller winglet at the bottom side of the wing). In contrast to Airbus who applies the wingtip fences by default on most of their aircraft (and the winglets on the A330/340 family), blended winglets are considered by Boeing for example as an optional extra feature on their products, except for the Boeing 747-400. For some of the older Boeing jets (737 and 757) such blended winglets have been offered as an aftermarket retrofit, these are the newer, tall designs and do not connect to the tip of the wing with a sharp angle, but with a curve instead. These winglets are popular among airlines that fly these aircraft on medium/long haul routes as most of the real fuel savings materialize while cruising. Longer flights mean longer cruising, thus larger fuel savings. They also server as marketing surface for airline logos or web addresses usually.



**Fig.11: blended winglets.**

### 3.10.3 Raked wingtips

They are the most recent winglet variants (they are probably better classified as special wings), where the tip of the wing has a higher degree of sweep than the rest of the wing. They are widely referred to as winglets, but they are better described as integrated wingtip extensions as they are (horizontal) additions to the existing wing, rather than the previously described (near) vertical solutions. The stated purpose of this additional feature is to improve fuel economy, climb performance and to shorten take off field length. It does this in much the same way as “traditional” winglets do. In testing by Boeing and NASA, raked wingtips have been shown to reduce drag by as much as 5.5%, as opposed to improvements of 3.5% to 4.5% from conventional winglets. Airliners to use raked wingtips: Boeing 747-8, Boeing 767-400ER, Boeing 777 (-200LR; -300ER; and freighter versions) plus the new Boeing 787 Dreamliner and the Airbus A350. The 747-8, the 787 and the A350 will have special, new kind of wings, which do not have a separate winglet, but have raked, and blended wingtips integrated without a sharp angle between the wing and the winglet.





**Fig.12: raked wingtips on the new Boeing 787 and Airbus A350.**

In the figure 13, reproduced below, different types of winglets can be seen. Basically, conventional blended winglet or blended winglet and elliptical winglet are very similar. It only changes the wingtip angle. Raked winglet is not very usual type of winglet.

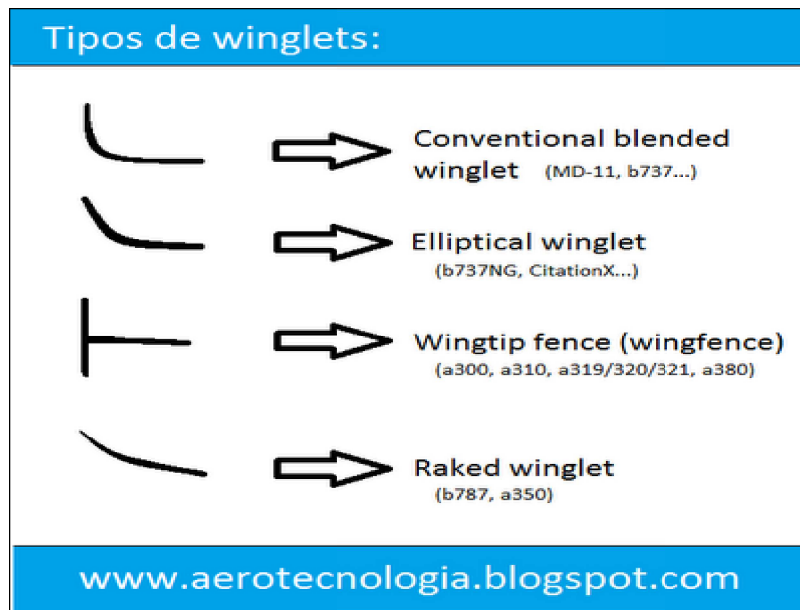


**Fig.13: types of winglets.**

### 3.11 Computational Fluids Dynamics (CFD)

Fluid mechanics is the branch of continuum mechanics (which in turn is a branch of physics) that studies the movement of fluids (gases and liquids) and the forces that cause them. The key feature that defines the fluid is its inability to withstand shear forces (causing lacking definite form). It also examines the interactions between the fluid and the boundary that limits.

The governing equations of fluid mechanics all are obtained by applying the conservation principles of mechanics and thermodynamics to fluid volume. To

generalize we use the Reynolds transport theorem and the theorem of divergence (or Gauss) for the equations in a form more useful for the Eulerian formulation.

The three fundamental equations are the continuity equation, the equation of momentum, and the equation of energy conservation. These equations can be integrated in their design or in differential form, depending on the problem. This set of equations given in differential form is also called Navier-Stokes equations.

There is no general solution to this set of equations due to their complexity, so that for each specific problem of fluid mechanics study these equations are looking for simplifications that facilitate the resolution of the problem. In some cases it is possible to obtain an analytical solution, so we have to use computer-generated numerical solutions. This branch of fluid mechanics is called computational fluid dynamics. The equations are: continuity equation [3.6], equation of momentum [3.12] and equation of energy conservation [3.13].

$$\frac{\partial}{\partial t}(\rho v) + \nabla \cdot (\rho v \otimes v) = \rho f + \nabla \cdot \tau \quad [3.12]$$

$$\rho \frac{D}{Dt} \left( e + \frac{1}{2} v^2 \right) = -\nabla \cdot (p v) + \nabla \cdot (\tau' \cdot v) + \rho f \cdot v + \nabla \cdot (\kappa \nabla T) \quad [3.13]$$

The Navier-Stokes equation describing the fluid motion and is related to the Reynolds number of fluid through the fluid viscosity, being  $\rho$  is the fluid density,  $v$  the velocity and pressure  $P$ .

The computational fluid dynamics (CFD) is a branch of fluid mechanics that uses numerical methods and algorithms to solve and analyze problems on the flow of substances. Computers are used to perform millions of calculations required to simulate the interaction of fluids and gases with surfaces designed for engineering complex.

Even with simplified equations and high-performance supercomputers, only approximate results can be achieved in many cases. Ongoing research, however, allows the incorporation of software that reduces the speed of calculation as well as the margin of error in analyzing situations while allowing more complex fluids such as transonic and turbulent flows. The verification of the data obtained by CFD is usually carried out in wind tunnels or other physical scale models.

The main elements in computational fluid dynamics (CFD) are:

-Discretization of continuous flow, the field variables ( $p$ ,  $v$ ,  $w$ ...) are approximated by a finite number of values at points called nodes.

-The equations of motion are also discretized approximate function values at the nodes.

-The systems of algebraic equations are solved and we obtain the values of the variables in the nodes.

The computational fluid dynamics has been used in a large number of engineering disciplines, such as aerodynamics, ship hydrodynamics, engines or combustion.

The results of a computational fluid study are similar to those we obtained experimentally in a wind tunnel: they both represent sets of data obtained from a given flow, with Mach number, Reynolds, etc. However, a wind tunnel is a very expensive, large, heavy and difficult to transport. In addition, requires the construction of a model, usually to scale, for study in the tunnel. With the use of computers, however, many of these problems become insignificant: we can design our object of study through computer design, and somehow, we have at our disposal a "transportable wind tunnel" always ready.

Another reason for using CFD is that while in an experiment can only take action in a limited number of points and instants of time, using a computer, we know the parameters we are interested at any point and instant of time.

In cases of research and development cost is a major factor is always taken into account and tries to minimize. Clear examples of this are the companies that are involved in Formula 1. The teams are constantly developing the cars, seeking improvements to enable win tenths of second per lap. The use of CFD allows them to perform many simulations with small variations on the same piece, and thereby to achieve an optimized solution. Otherwise, for each variation should build and test piece, with the cost that this entails.

There is a real example that illustrates the advantages of CFD. The Formula-1 Renault F1 team last year 2009 bought a supercomputer capable of performing 38 trillion operations per second. This is the Xtreme-X Supercomputer. According to Renault the cost is 50% of a real wind tunnel, a figure that may be around 20 million €, but just start it already provides 50% of the proceeds of a mature plant.

## **4 EXPERIMENTAL PROCEDURES**

### **4.1 Solid Edge v18**

Solid edge v18 is a kind of software created and dedicated to draw very easy in 3D. The wing model without winglet and the three wings models with winglets have been designed in solid edge v18. Circular winglet, blended winglet and wingtip fences have also been built. In order to do that, an airfoil section was picked as well as a data file was created with the airfoil points. To work in solid edge v18, it was previously necessary to create a excel table with the lower and upper surfaces airfoil points. By the time where the wings were finished, they were automatically exported to Gambit 2.4.6 in “step” format. When you export into “iges” format, volumes can not be exported; therefore you need to get them generated in Gambit 2.4.6. A naca 2415 airfoil was chosen to develop my wings. Later on, I used that airfoil at the wing root airfoil and at the wing tip airfoil. I found it impossible to make a research regarding the A330 airfoil so I chose that type of naca airfoil, especially since it is used in similar aircrafts. After that, a symmetrical naca airfoil 0012 was used to drawn blended winglets and wingtip fences. A symmetrical airfoil must be used because we do not want a high drag coefficient linked to the winglet. So I finally tried to draw an Airbus 330-300 wing. In the figure 14, reproduced below, can be seen A330-300 general dimensions.

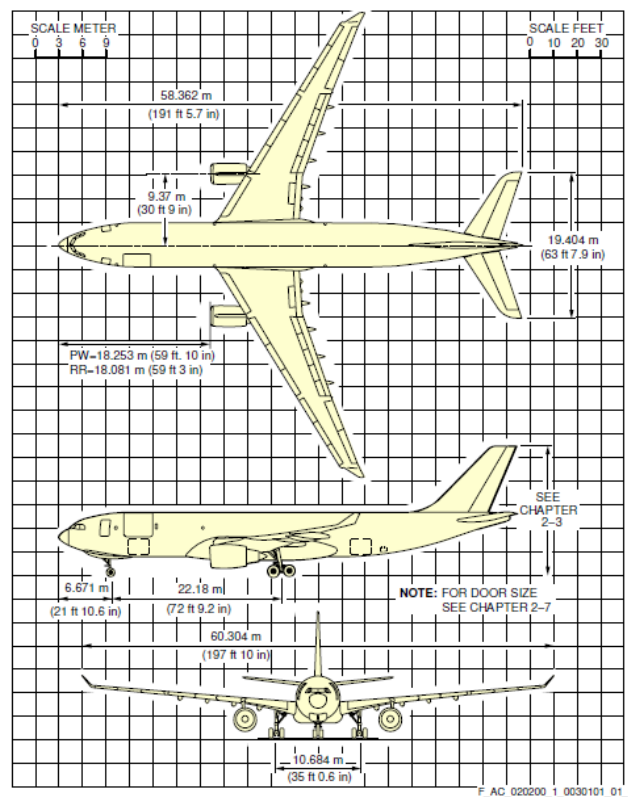


**Fig.14: A330-300 general dimensions.**

The images, reproduced below, show naca 2415 airfoil.

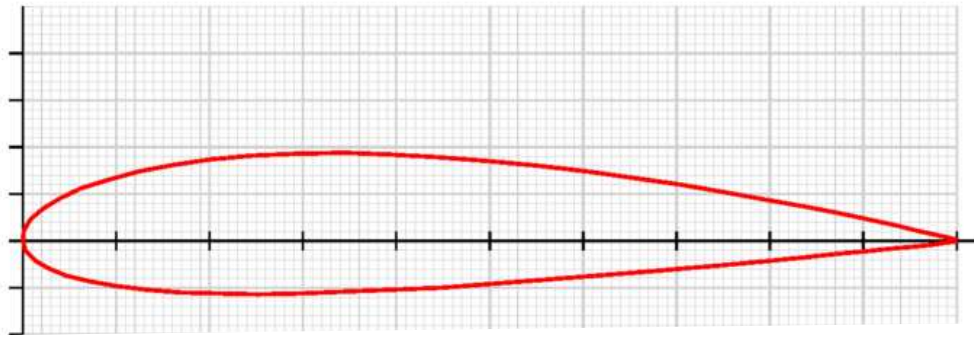


**Fig.15: naca 2415 airfoil.**

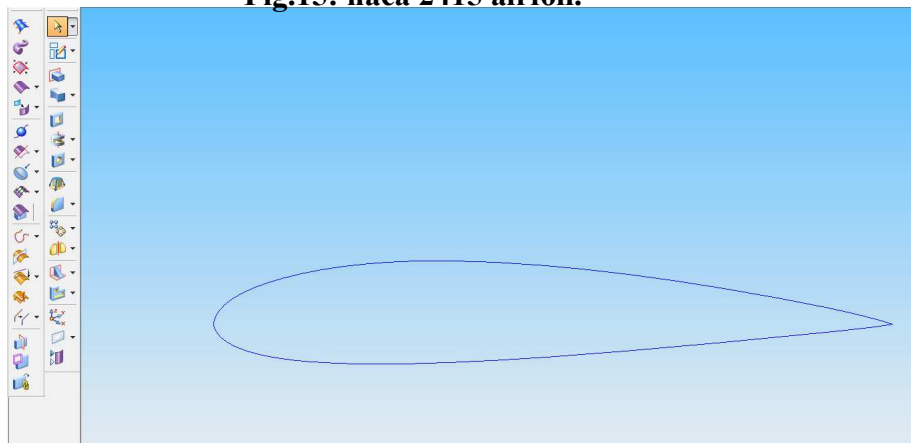


**Fig.16: naca 2415 airfoil in Solid Edge v18.**

When I got my airfoil into Solid Edge v18, the rest of the wing model was drawn. To do that, I had to shift and scale the initial airfoil to build my wing model. Four new airfoils were created, figure 17. It was difficult, as we can see in figure 14, wings dimensions are not very clear. When the airfoils were placed at the correct place, regarding the sketches we have previously shown, extrusion of sections option in Solid Edge v18 to sketch A-330 wing was used. The wing model before used extrusion of sections option is in figure 17. Wing completed is in figure 18.

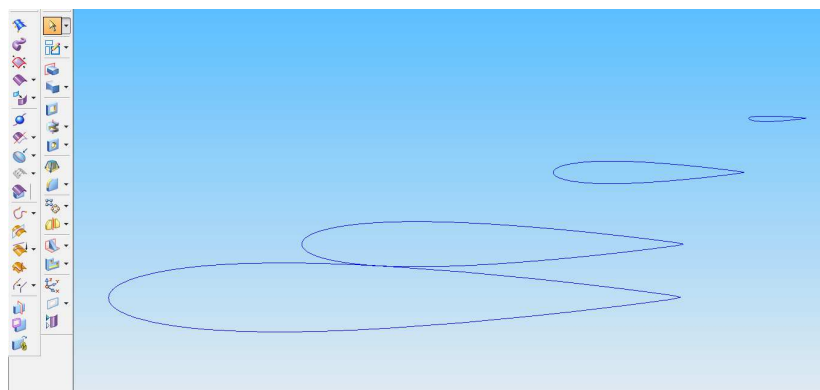


**Fig.17: wing model construction.**

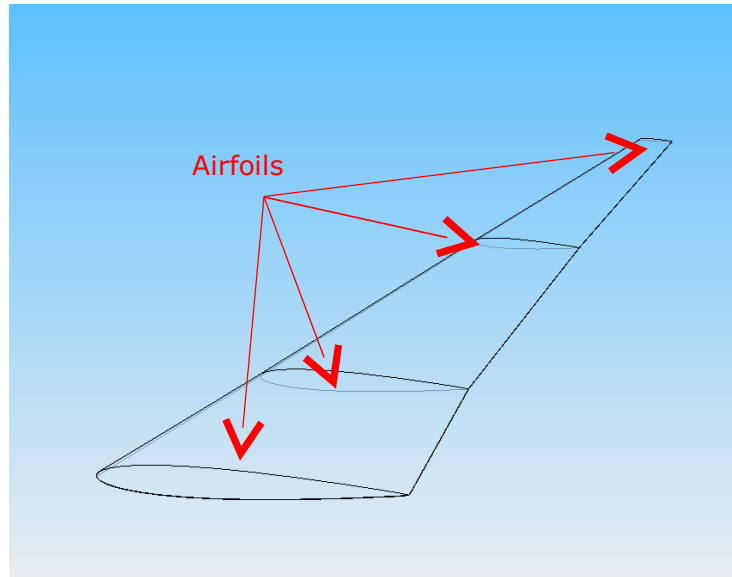


**Fig.18: wing model completed.**

Until now, all we have done is drawing the wing model without winglet. The process of sketching blended winglet model and wingtip fence model are quite similar. In the following figures, we can see the wings with blended winglet and wingtip fence completed.

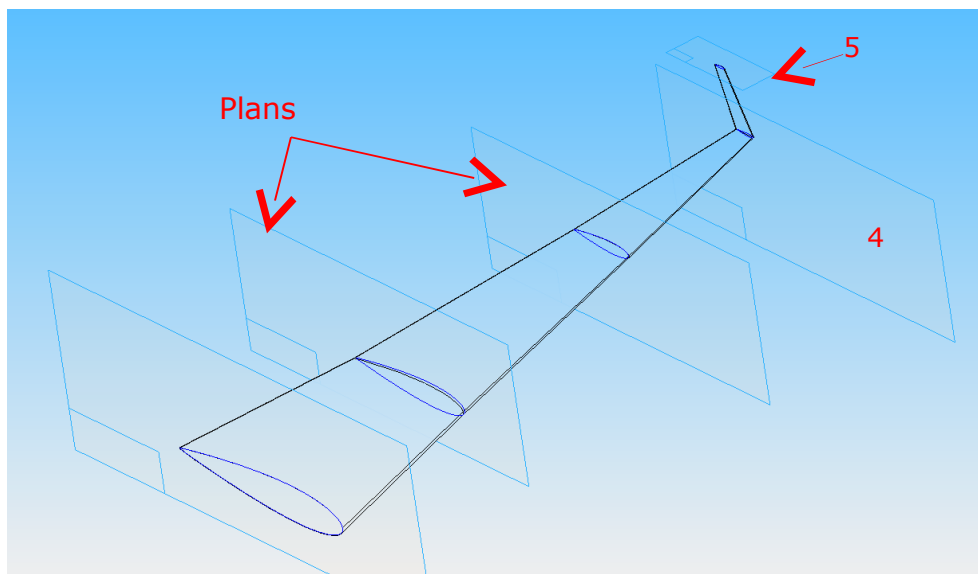


**Fig.19: wing model with blended winglet completed.**

In the figure 19, reproduced above, we can see the five plans and the different airfoils to draw wing with blended winglet. The angle between wing tip and winglet is almost  $90^\circ$ . Therefore, the angle between plan four and plan five is the same. The figure 20, reproduced below, shows the naca airfoil used to build the blended winglet.

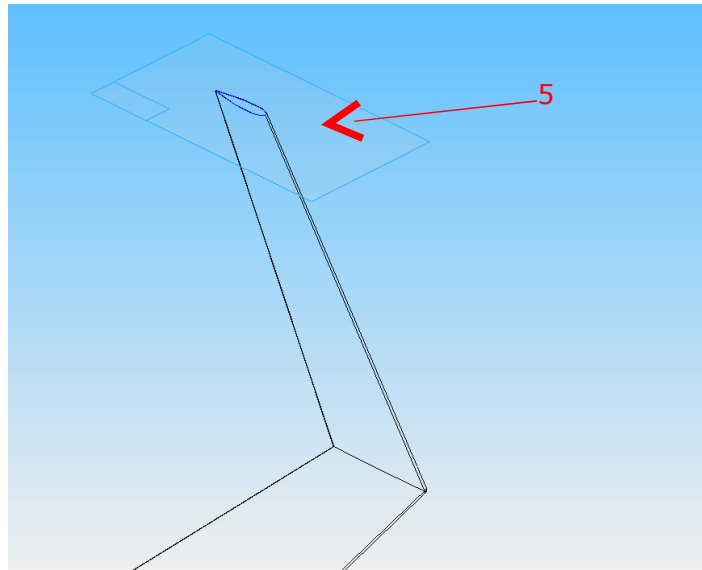


**Fig.20: blended winglet model zoom.**

In the figure 21, reproduced below, it can be seen the wing with wingtip fence completed and the plans 5 and 6 used to create wingtip fence.

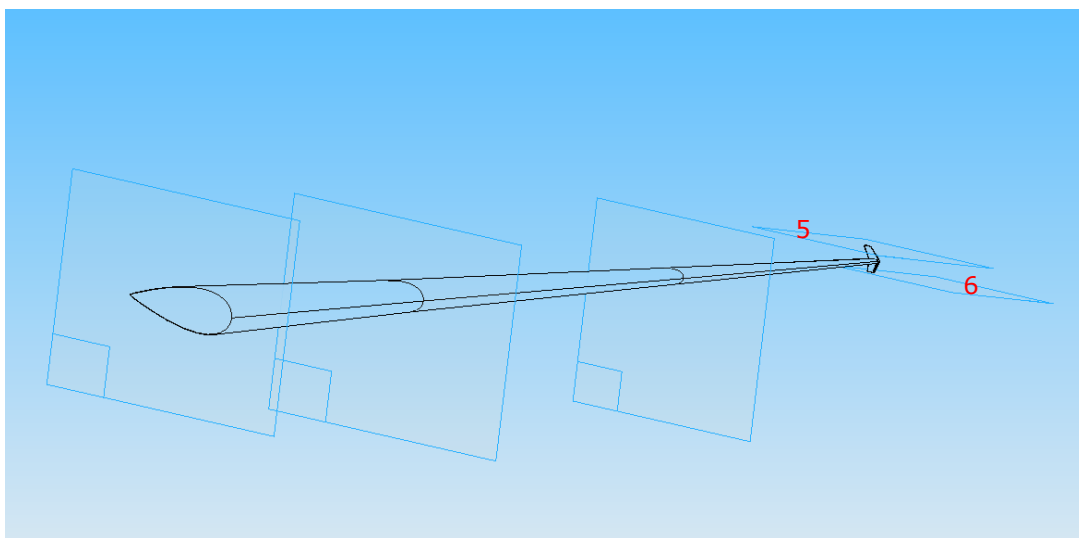


**Fig.21: wingtip fence model completed and plans.**

Now, I would like to talk about the last winglet. That winglet is a circular winglet. The process to build it is very similar. However, the airfoil winglet is not the same. A circular profile was created at the wingtip and extrusion for sections option in Solid Edge v18 was used to draw the wing with circular winglet, again. In the figure 22, can be seen the wing completed and the circular profiles. There is a circular winglet zoom in the figure 23. At the end of the next page, there will be a table with the wing areas.



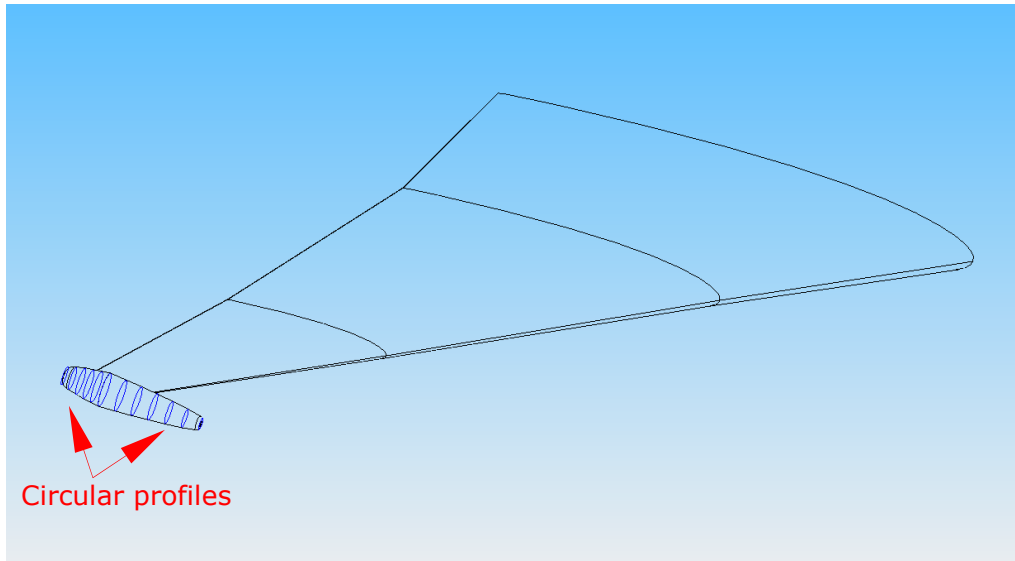


**Fig.22: circular profiles and wing model completed.**

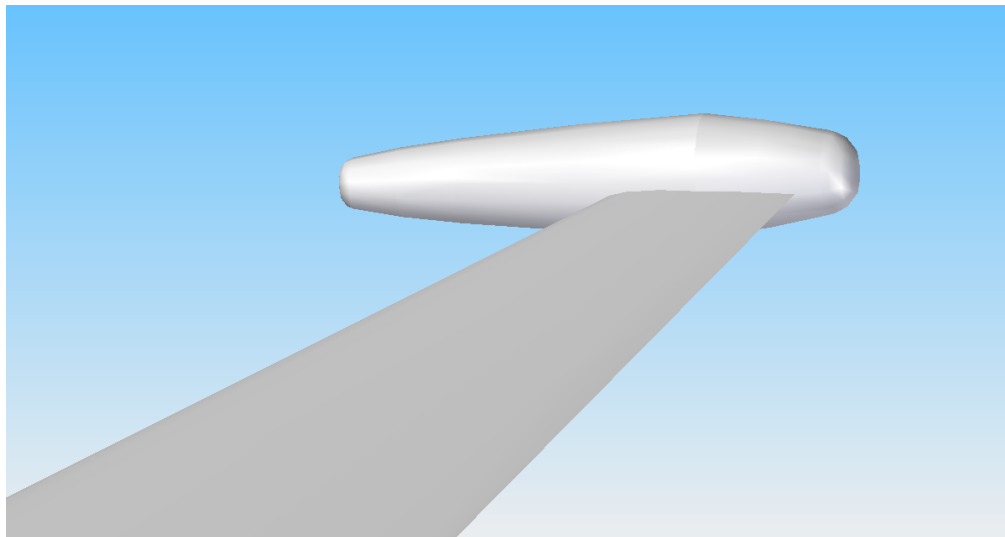


**Fig.23: circular winglet model zoom.**

Wing	No winglet	Circular winglet	Wingtip fence	Blended winglet
Area ( $m^2$ )	321.96	328.32	323.4	325.97

**Table.1: wing areas.**

These wing surfaces will be used to work out drag coefficient,  $C_d$ , lift coefficient,  $C_l$ , and lift and drag force. These wing surfaces have been calculated in two different ways, Solid Edge v18 and Fluent. In Fluent, I have used *report* → *surface integrals* option, *report type* → *area*, and in surfaces wing was picked.

#### 4.2 Gambit 2.4.6

Gambit is modelling software that is capable of creating meshed geometries that can be read into FLUENT and other analysis software. The different wings have been created. Importing the wings is the next step. When the wings are into Gambit 2.4.6 the control volume can be defined. The control volume will be wind tunnel. The dimensions control volume are; 50 m in x, 30 m in y and 40 m in z. To measure vorticity magnitude seven control zones will be created. Those control zones are circular and there is a space of three meters between each circle. The radius circle is five meters. The control zones are located at the same distance in all my wings models. That distance is 2 m from wingtip. The control zones are placed as the following figure show.

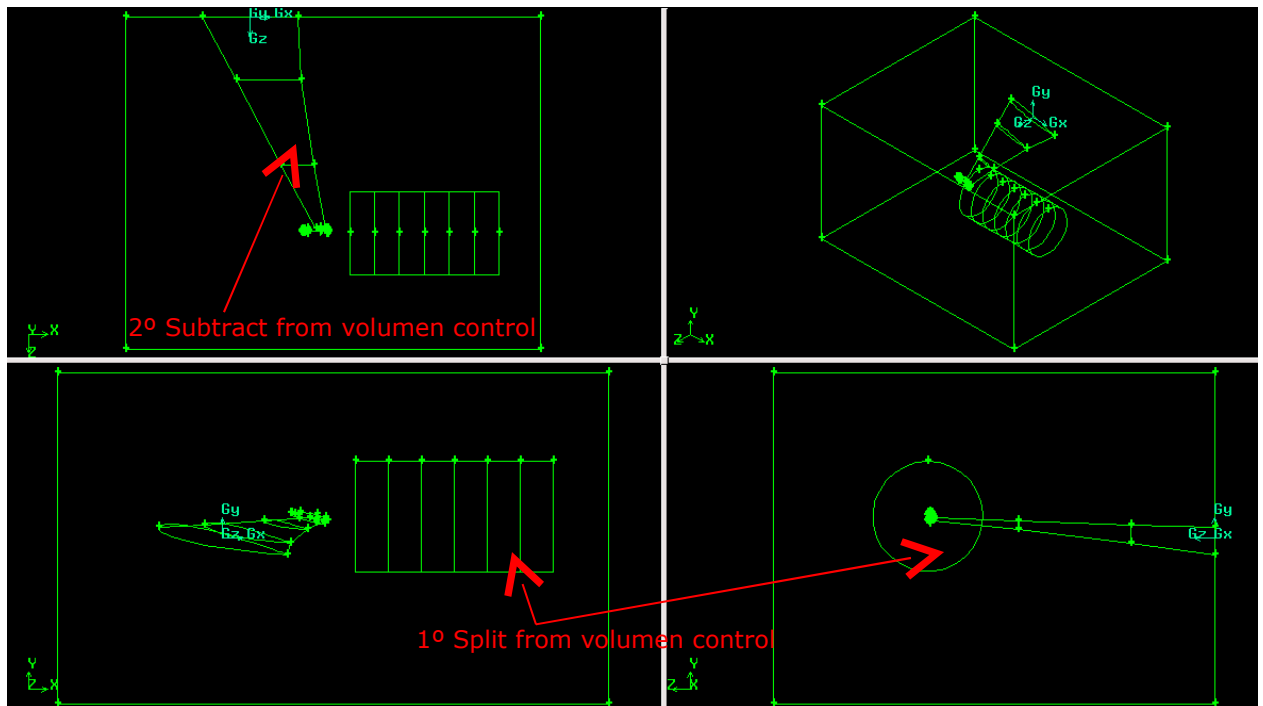


**Fig.24: control zones and wind tunnel circular winglet 12°.**

The following tasks were made in Fluent; First, I had to split control zones from control volume and second, I had to subtract wing models from control volume, as can be seen from figure 23. The rest of the wings are placed in the same place and the control zones and wind tunnel have the same dimensions. At this point, we discretized our geometry: this is the process known as meshing. What we can finally get is to move from a continuous to a discrete volume on which to solve the equations necessary to find the problem solution.

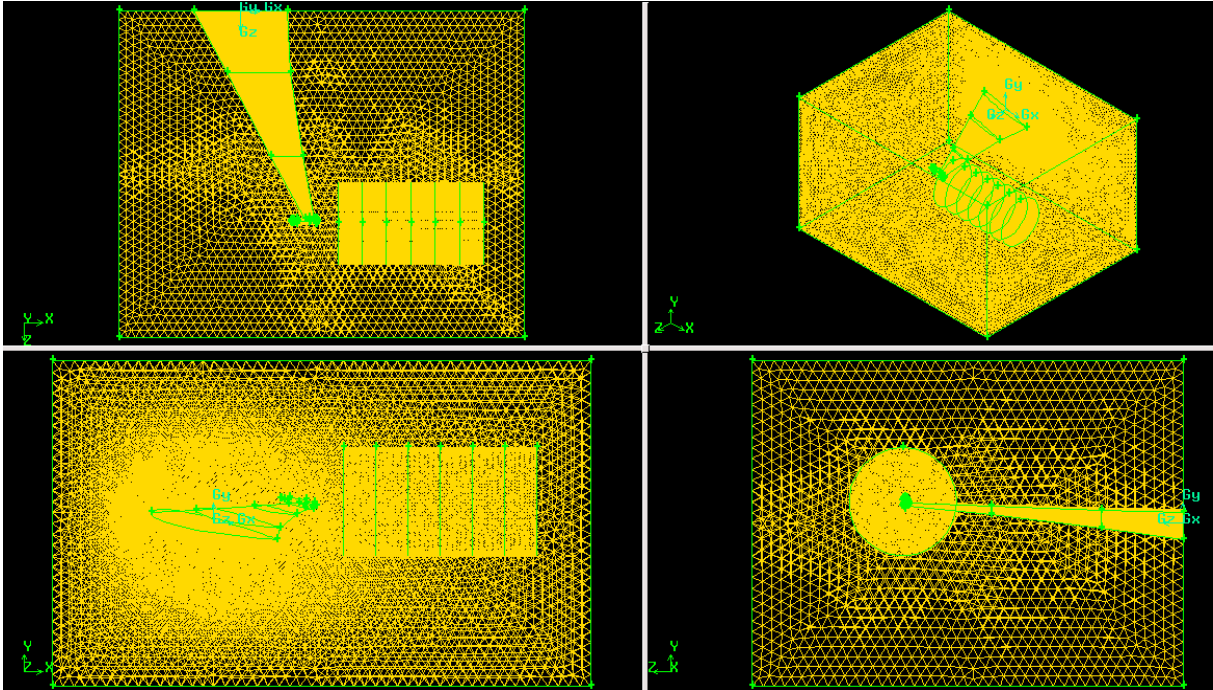


**Fig.25: mesh circular winglet 12°. Interval size 1.5.**

To create the mesh, tet/hybrid elements were used. First, I meshed the wing (face) with tri/pave elements, figure 25. Second, zone controls (face) were meshed with tri/pave elements too, figure 26. Between one control zone and seven control zone (volume) I meshed with tet/hybrid elements, figure 27 and finally wind tunnel were meshed with tet/hybrid again, figure 24. On the blended winglet and wingtip fence, I used a very fine mesh since the faces of these winglets are small and thin. The number totals of elements are about 1500000 depending on the type of winglet. The aspect ratio is between 1 and 4 in all my models.

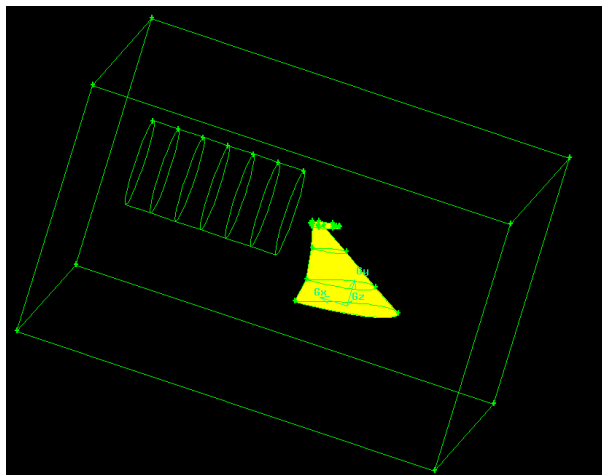


**Fig.26: wing mesh. Interval size < 0.1 depending on winglet.**

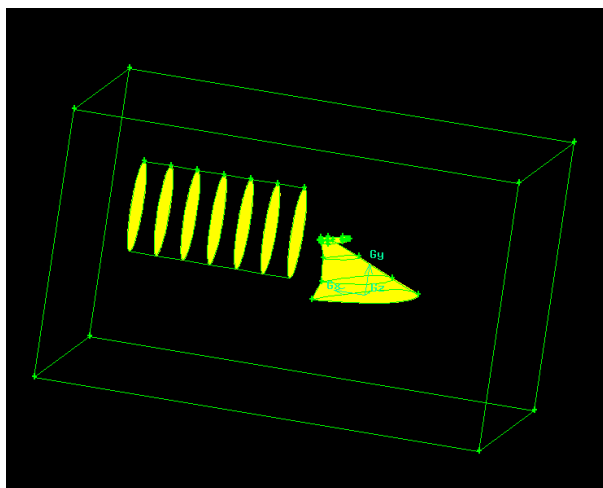


**Fig.27: control zones mesh. Interval size 0,3.**

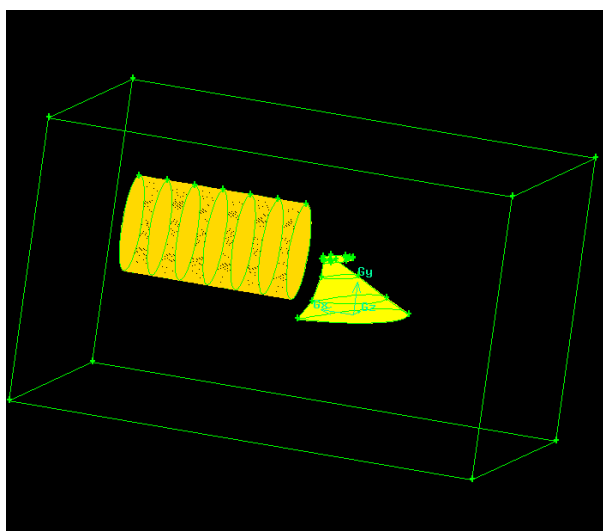


**Fig.28: volume control zones mesh. Interval size 0,5.**

#### 4.3 Fluent 6.3.26

The desired mesh can now be read into FLUENT which will then run the geometry through the numerical analysis. Different angles of attack will be analyzed in Fluent 6.3.26. The maximum wingtip vortex is produced when the aircraft's velocity is low, therefore the winglets will be studied when the aircraft is taking off with different angles of attack between 0 and 16 degrees. To measure vorticity magnitude behind wing, seven control zones have been created. They are interior and their colour is green, figure 28 and 29.

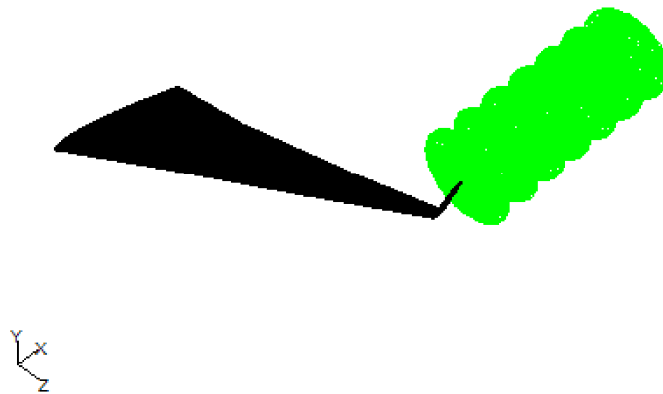


**Fig.29: control zones blended winglet 8°. Isometric view. Orthographic projection.**

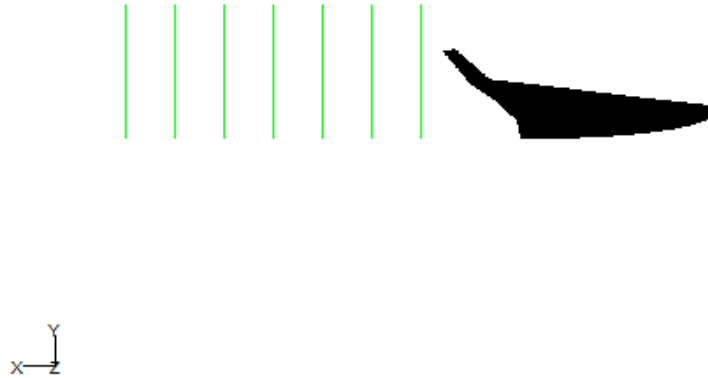


**Fig.30: control zones blended winglet 8°. Back view. Orthographic projection.**

I am ready to start my CFD analysis of winglets. It is necessary to talk about the set of values used in Fluent 6.3.26. K-epsilon viscous models was picked since it is a two equation model that works very well in these kinds of problems. The velocity inlet is 77.78 m/s ( $M=0.228$ ). To compute drag coefficient and lift coefficient I have to go to reference values into Fluent and the length will be 29.05 m and the area depends on the winglet. The different areas can be seen from table 1. Basically, vorticity magnitude and drag coefficient must be calculated to compare the performance wing model without winglet and with winglets. The solution is converged as a result of among 140 and 200 iterations.

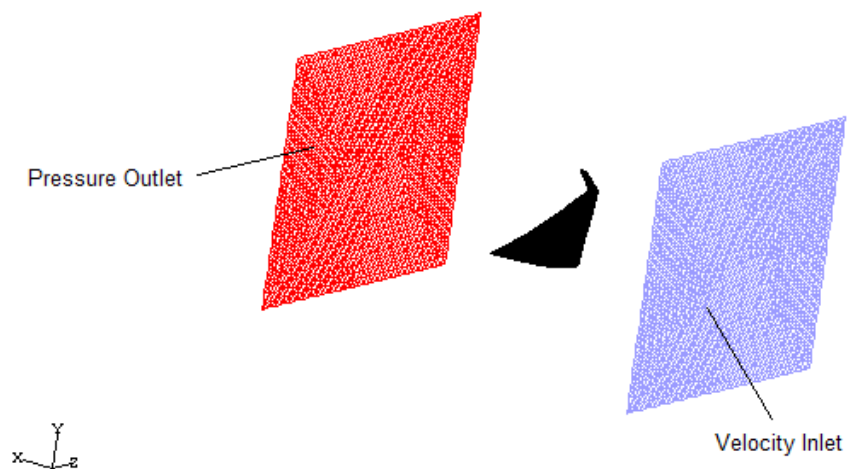


**Fig.31: grid blended winglet 8° I.**

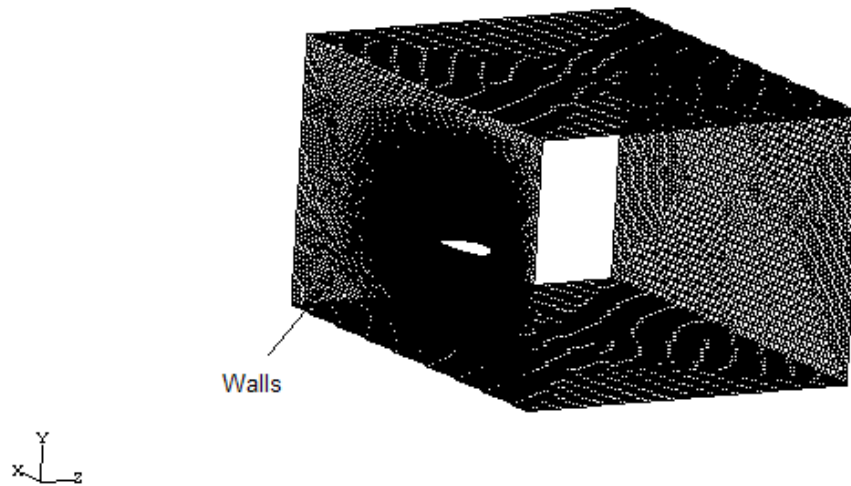


**Fig.32: grid blended winglet 8° II.**

## 5 RESULTS AND DISCUSSION

In this section, results from Fluent will be shown and discussed. Wingtip vortex development and performance will be checked in the first part of this section. To do that, we are going to study the different wings from several angles of attack between 0 and 16 degrees. In addition to that, an attempt to explain why wingtip vortices are broken or reduced will be made. We know wingtip vortex is turning around on its own axis and that axis begins to nearby the wingtip. Furthermore, wingtip vortices spin anticlockwise in my models and the axis in which wingtip vortex is developed moves down and laterally when the vortices are away from wingtip. Vorticity magnitude is related to lift so the wingtip vortex intensity will be checked when the lift increases. Finally, a summary table will be showed in which the drag coefficient improvement can be compared. The set of results will be given in several tables, diagrams or figures.

### 5.1 CFD Analysis of wingtip vortices development

To study wingtip vortices development, wing model without winglet will be used with an angle of attack of 0 degrees and with angle of attack of 4 degrees. With an angle of attack of 0 degrees, my wing model without winglet is not able to generate an enough lift coefficient to develop wingtip vortex. In fact, the drag coefficient is higher than the

lift coefficient at 0 degrees. Lift coefficient,  $C_l$ , at 0 degrees is equal to 0.0006456 and drag coefficient,  $C_d$ , at 0 degrees is equal to 0.009584, therefore the ratio  $C_l/C_d$  is equal to 0.06736. Despite the fact  $C_d$  is higher than  $C_l$ , the aircraft will not have any problems to start out taking off, especially since spoilers and flaps are used by aircraft's pilots to improve wing's  $C_l$  at that moment. Moreover, an aircraft flies just when it can produce enough lift force to win gravity force. As we can see in section 3.8 called wingtip vortex development, vortices tend to form thanks to the difference in pressure between the upper and lower surfaces of a wing, which is operating at a positive lift. Thus, there will not be vortices behind my wing at 0 degrees.

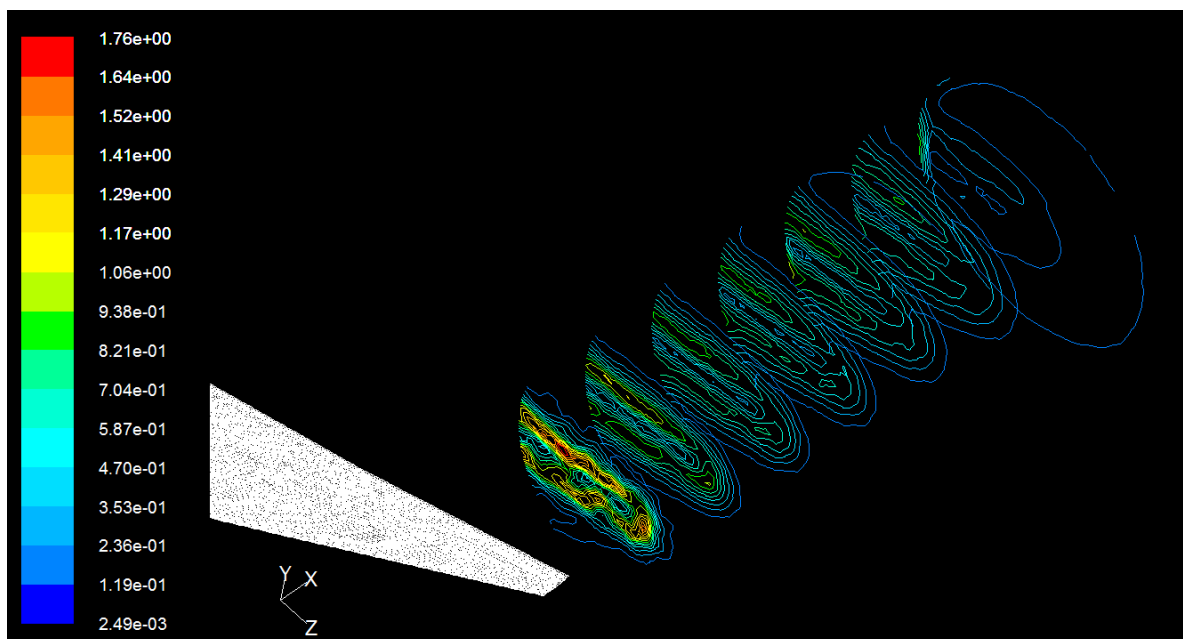
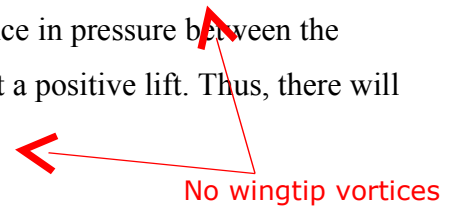


**Fig. 33: contours of vorticity magnitude (1/s) at 0° in control zones. No winglet.**

As we can see in figure 32, there are no real wingtip vortices created perfectly. Moreover, there is no axis in which vortices can spin. In the next figure, wingtip vortices and its axis can be checked.



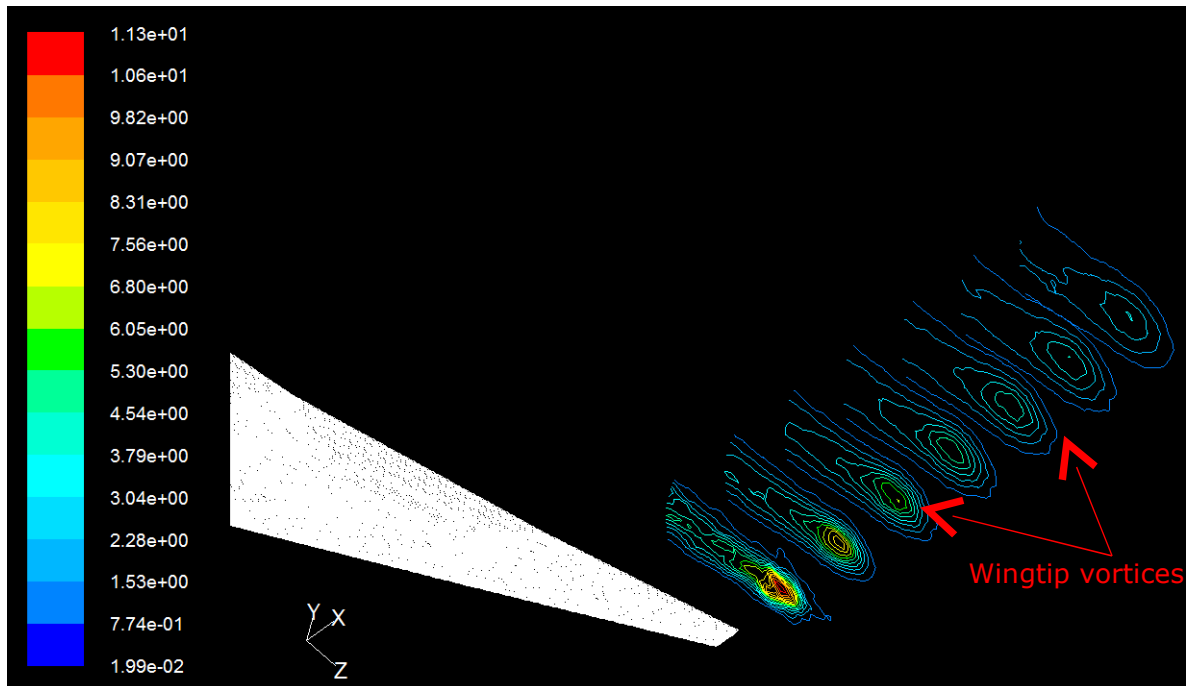


**Fig.34: contours of vorticity magnitude (1/s) at 4° in control zones. No winglet. Orthographic projection.**

The figure 33, reproduced above, shows vorticity magnitude in control zones with an angle of attack of 4 degrees. With that angle of attack, the value of  $C_l$  equals 0.16036 and the value of  $C_d$  equals 0.01461 and then, the value of  $C_l/C_d$  equals 10.974. My wing model without winglet is able to generate a positive lift and therefore, wingtip vortices can be developed, as can be seen from the figure 33. With the rest of the wings models takes place in the same way, I mention that to show that, at 0 degrees there is no wingtip vortices, since the wings are not operating at positive lift. Besides, the ratio  $C_l/C_d$  is less than 1. From 0 degrees, as the ratio  $C_l/C_d$  is higher than 1 there is wingtip vortices development. A wing generates wingtip vortices, as it is able to produce a ratio  $C_l/C_d$  higher than 1.

Vortices form due to the difference pressure between the lower and upper surface in a wing. As my wing model works at 0 degrees, there is no difference pressure between lower and upper surface and so there is no lift and no wingtip vortices. The difference pressure between lower and upper surface in a wing generates lift and therefore wingtip vortices. A new surface has been created to calculate the pressure difference in the wingtip. The following figures show the new surface created and the difference pressure in the wing model, when it is working at 0, 4, 8, 12 and 16 degrees. At 4 degrees, the

difference pressure between lower and upper surface is higher than at 0 degrees, and that difference pressure gets higher at 8 degrees. Of course, when the angle of attack increases the difference pressure goes up too.

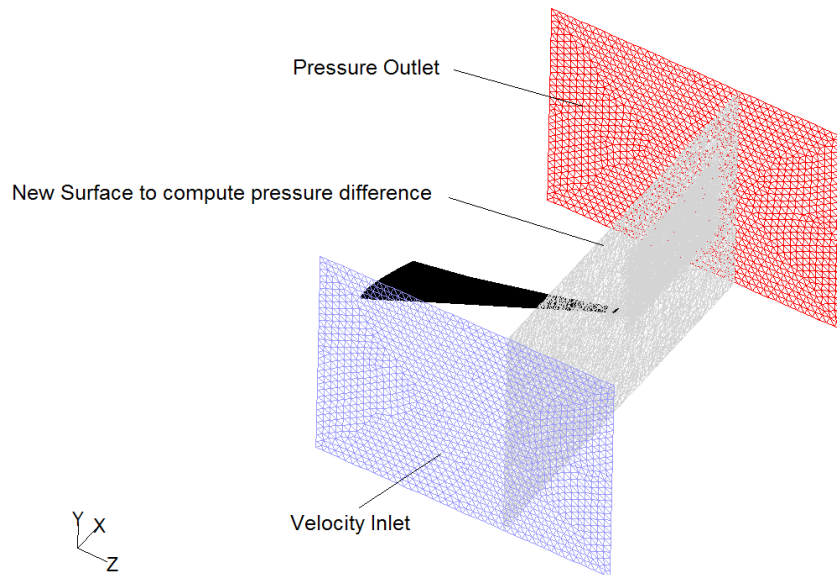


**Fig.35: surface at wingtip to work out pressure difference. Perspective projection.**

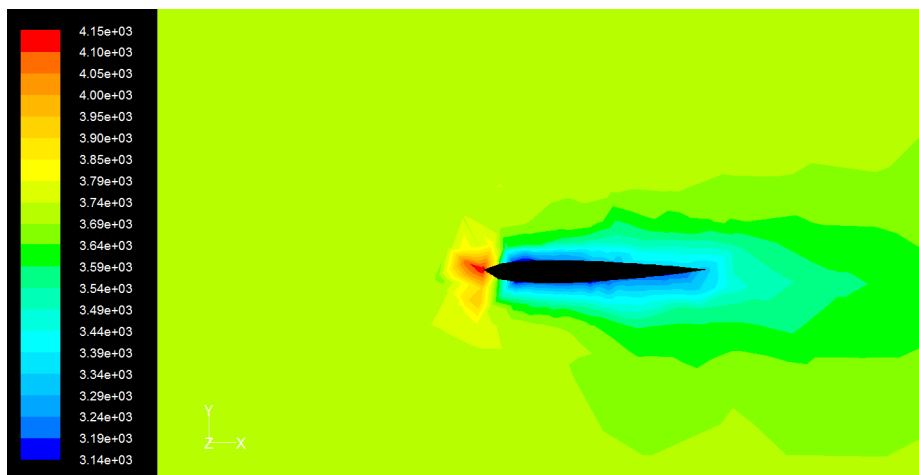


**Fig.36: contours of total pressure (Pa) 0° no winglet at wingtip.**

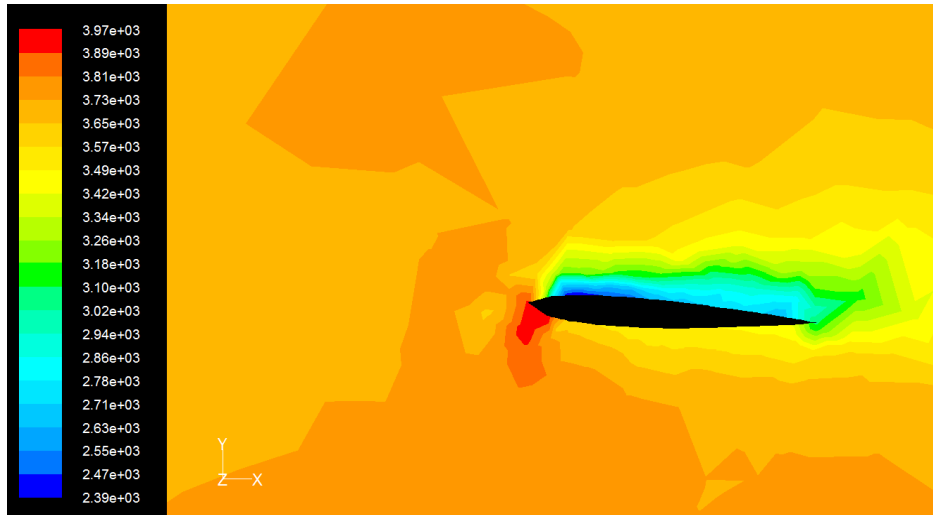


**Fig.37: contours of total pressure (Pa) 4° no winglet at wingtip.**

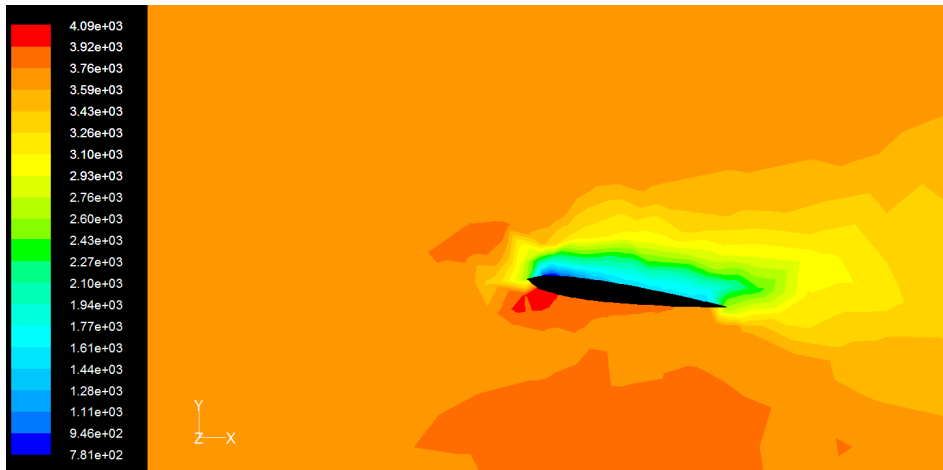


**Fig.38: contours of total pressure (Pa) 8° no winglet at wingtip.**

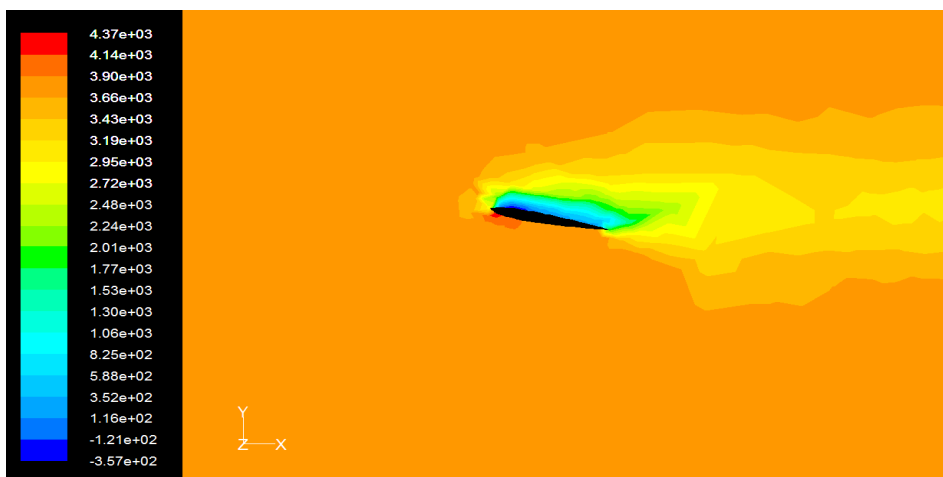


**Fig.39: contours of total pressure (Pa) 12° no winglet at wingtip.**

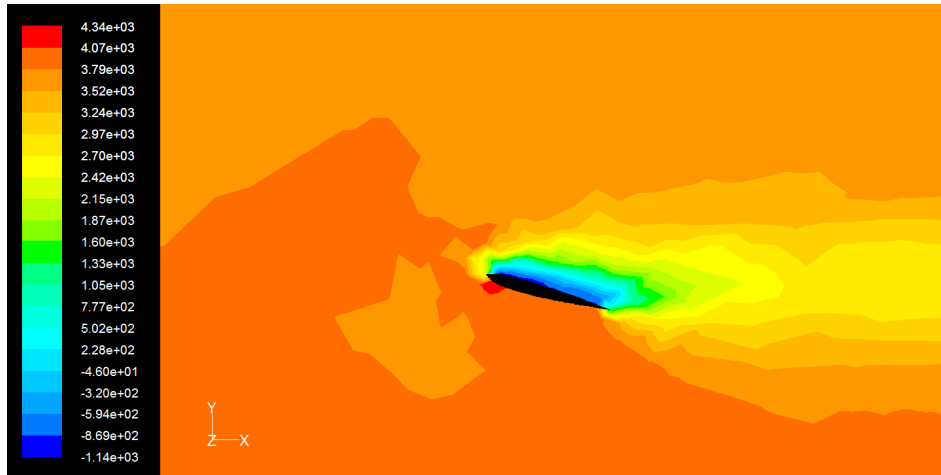


**Fig.40: contours of total pressure (Pa) 16° no winglet at wingtip.**

## 5.2 CFD Analysis of wingtip vortices performance

Until now, we have seen when and why the wingtip vortices are developed. In the next pages, I would like to talk about vortex rotation and how the vortex moves down and goes sideways when it gets away from wingtip. In the figure 39, reproduced below, we can see wingtip vortex performance. We should keep in our minds, my wings models are placed on the right of the aircraft, so the vortex rotation moves anticlockwise from a front view. Lower surface is the zone where the pressure takes its highest value, and also in the upper surface the value of pressure is smaller than lower surface, figure 34

until figure 38. The air goes up from the lower and upper surface and then, the wingtip vortices spin anticlockwise.

On the other hand, the vortex axis starts out at the same height as the wingtip or winglet tip and its axis moves down and up. Furthermore, the vortex axis moves away sideways from the wingtip.

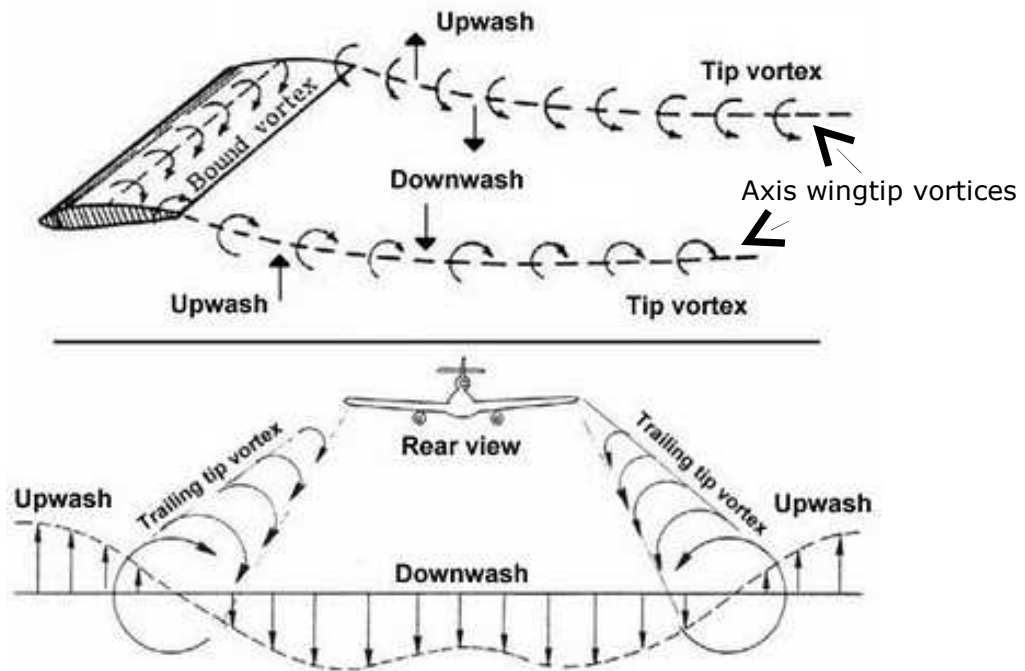
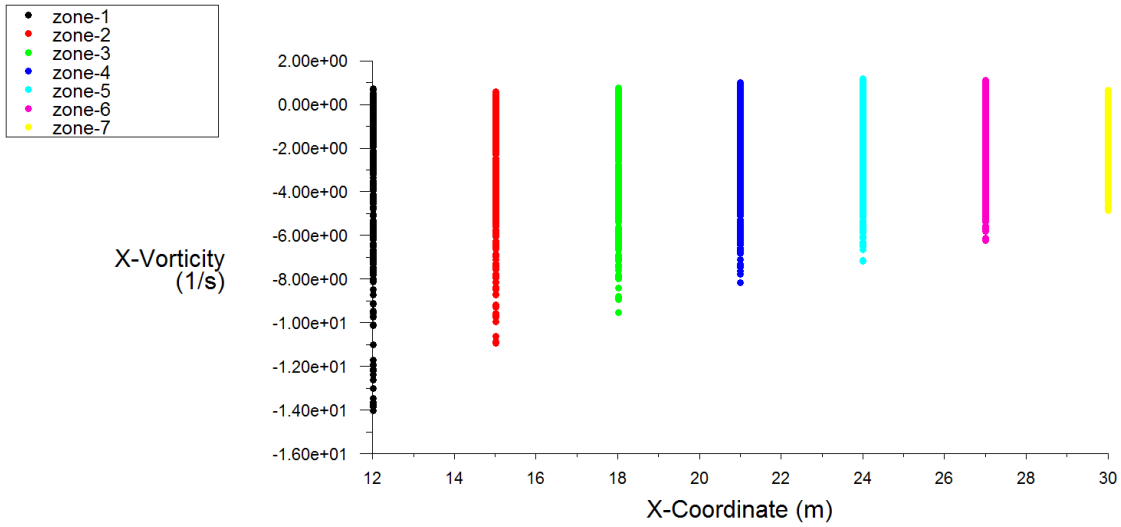


**Fig.41: wingtip vortex performance.**

To study wingtip performance, circular winglet will be used to check vortex rotation and wing model with blended winglet will be used to check wingtip vortices axis location. Such model is very appropriate to check how the axis vorticity moves down and up and for that, it has been picked. We are going to start vortex rotation and this section will be finished talking about axis location.

### 5.2.1 Vortex rotation

To measure vortex rotation, a graph will show in the Y axis the value of velocity x-vorticity and in the X axis grid x-coordinate. The control zones are the ones to study. In the graph 1, we can see the separation between each control zone is 3 meters. We can also see how the values of velocity x-vorticity decrease as control zones get away from wingtip. The values in Y axis have negative signal which means vortices spin anticlockwise.



**Graphic.1: X-Vorticity vs. X-coordinate .Circular winglet 8°.**

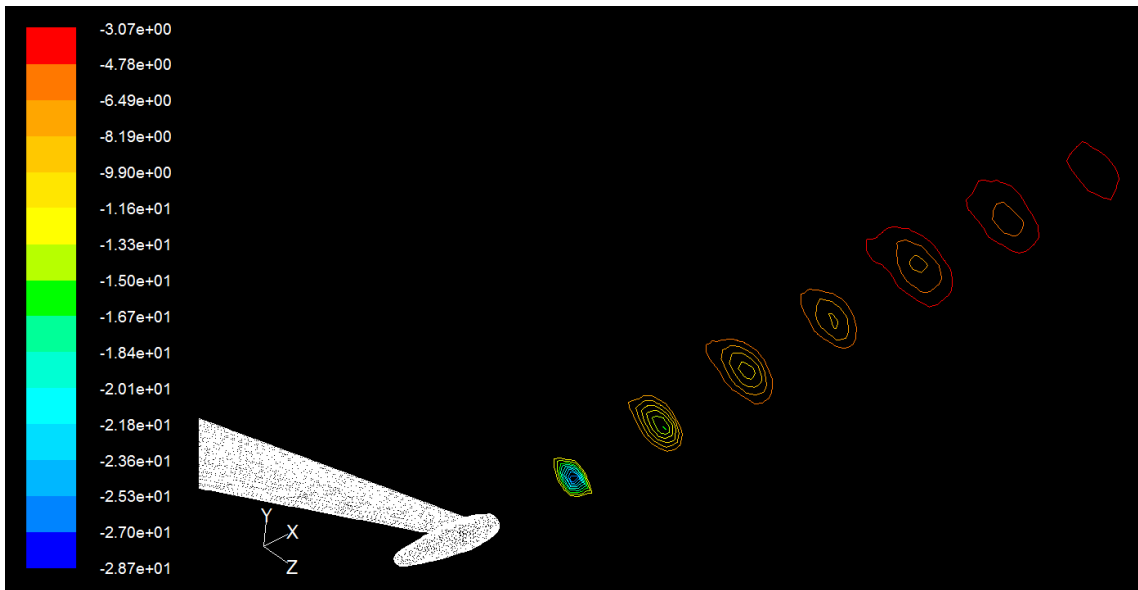


**Fig.42: contours of X-vorticity (1/s) iso-clip surface. Circular winglet 8°. Orthographic projection.**

If we use the "right hand" rule of directions in order to know which oriental direction gets our function, we can see the values situated up get the strongest negative signals and the other way round with the ones which are down, weakest negative signal. In the figure 41, iso-clip surface option into Fluent has been used to adapt control zones, and thus we can check better the vortex rotation. In the next figure, we can see the seven control zones without iso-clip surface option used into Fluent.

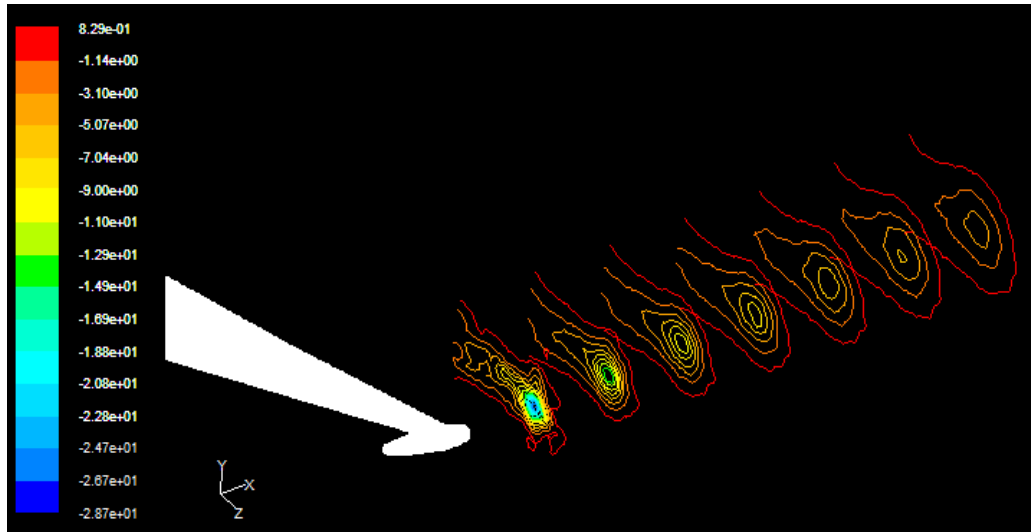


**Fig.43: contours of X-vorticity (1/s). Circular winglet 8°. Orthographic projection.**

### 5.2.2 Wingtip vortex motion

In this section, we are going to use wing model with blended winglet with an angle of attack of 4 degrees to check how axis wingtip vortices and therefore, wingtips vortices move down and up. To do that, it is absolutely necessary to know reference system which will be use to demonstrate wingtip vortices motion. With the grid X-coordinate, we can move left to right on the sheet plane. With the grid Y-coordinate, we can move down to up on the sheet plane. Finally, the grid Z-coordinate means a perpendicular sheet plane. I hope that next figures help to understand using coordinates when they are in different graphs. In the figures 42 and 43, we can see the grid X-coordinate direction and the grid Y-coordinate direction. It is not possible to see the grid Z-coordinate direction since it is perpendicular to sheet plane. Furthermore, seven control zones can be seen.

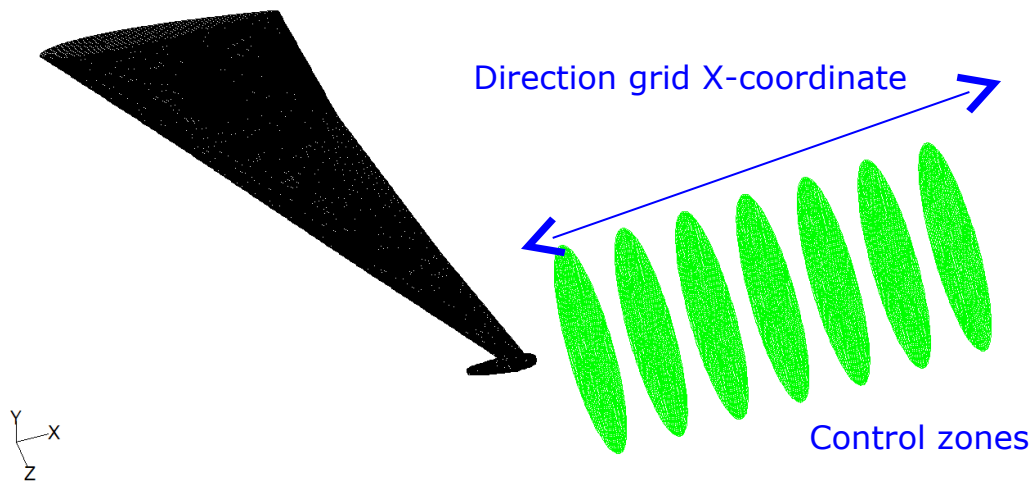


**Fig.44: reference system. Orthographic projection.**

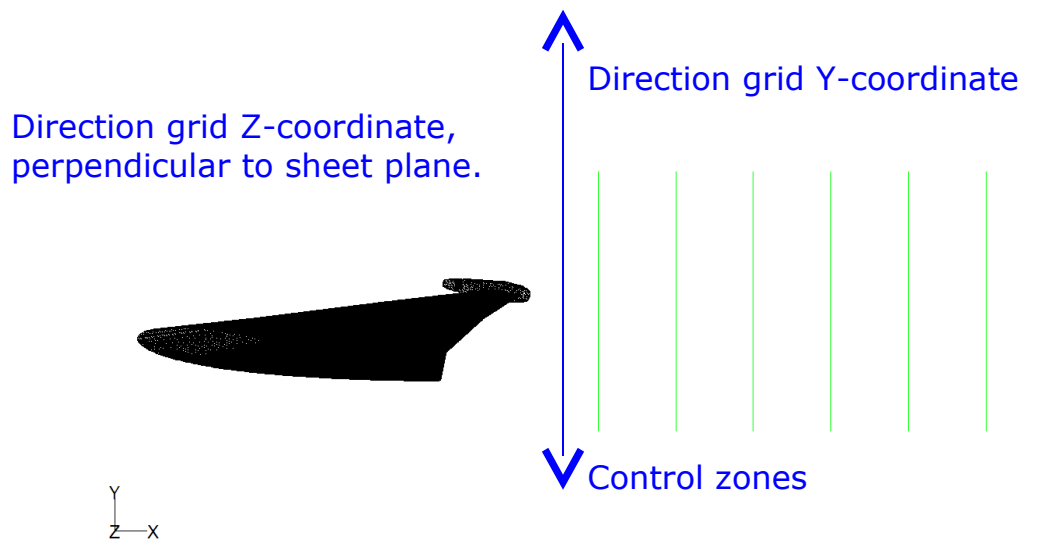


**Fig.45: reference system. Front view. Orthographic projection.**

The reference system has already been explained, so we are ready to start out to check wingtip vortex motion. To study how wingtip vortices move down and up, a new surface close to wingtip will be created. Also, the seven control zones are used. We can see the vorticity magnitude in the new surface created in the figure reproduced below, figure 44. The wing model is one which blended winglet linked to wingtip.



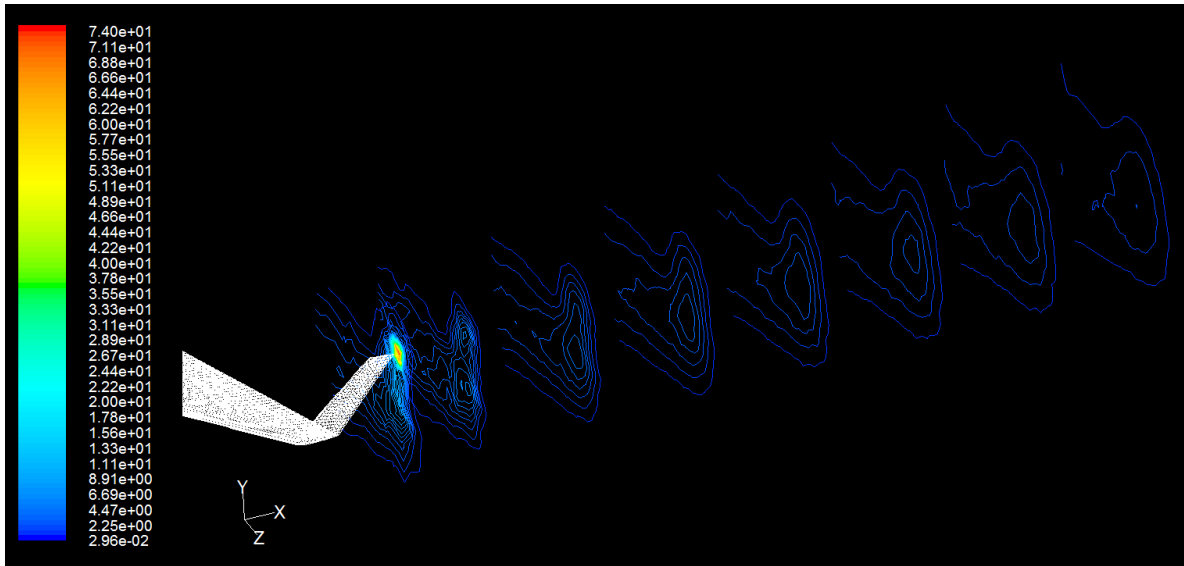
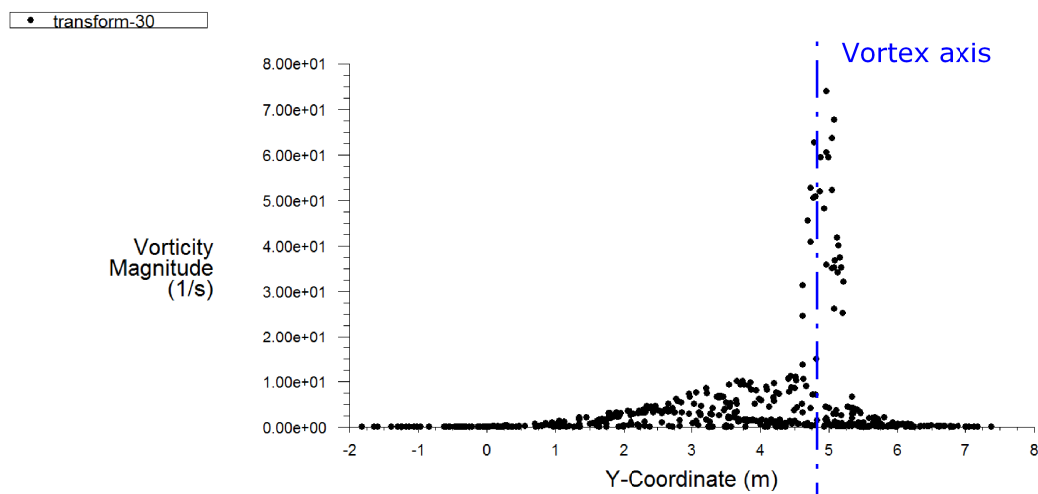
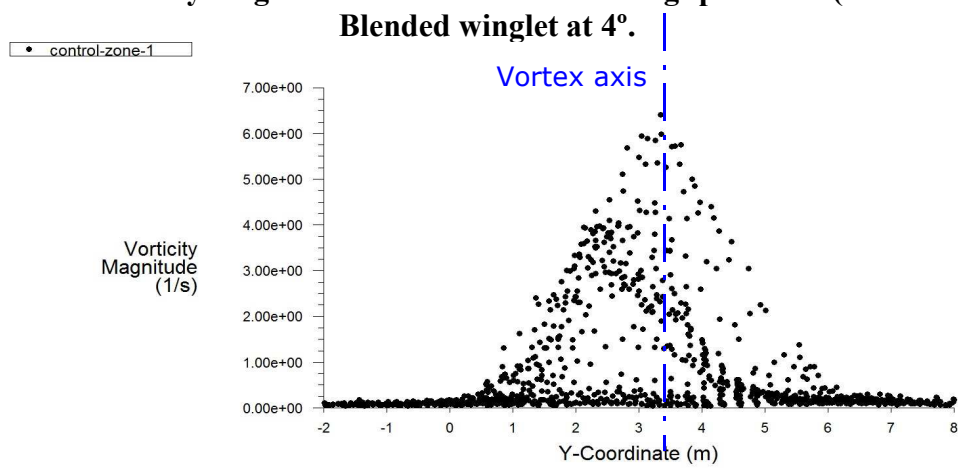


**Fig.46: contours of vorticity magnitude (1/s) blended winglet at 4°. Orthographic projection.**

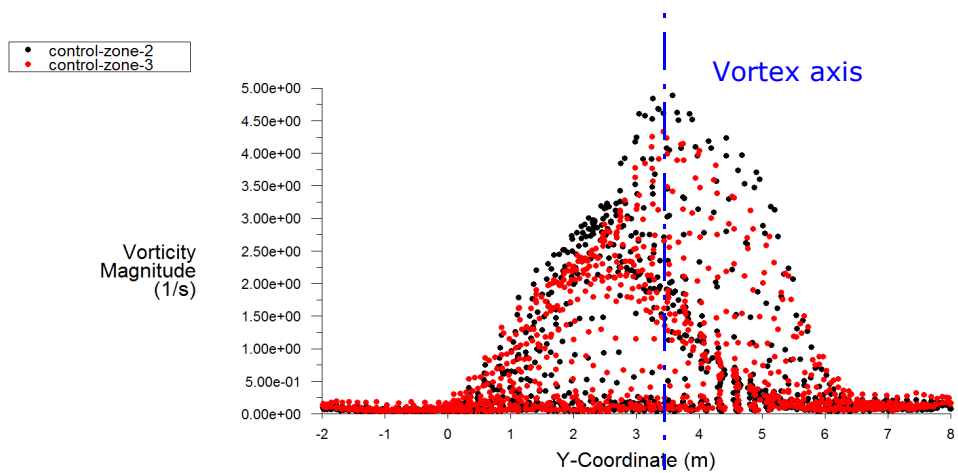
We can see from figure 44, the vortex is placed at the wingtip in the first plane. As we move away from wingtip, the wingtip vortex moves down. Furthermore, the vortex lost intensity. In the next graphs, we can see where the vortex maximum value and, where is placed such maximum value. The maximum value is placed into the wingtip vortex axis. Remember, wingtip vortex is turning around on its own axis. Also, we can see vortex widens as it moves away from the wingtip. The following graphs show the vorticity magnitude (1/s) versus grid Y-coordinate at the wingtip plane and the seven control zones. The graphic 8 shows where wingtip surface and control zones are placed in grid X-coordinate, as well as maximum value of vorticity magnitude.



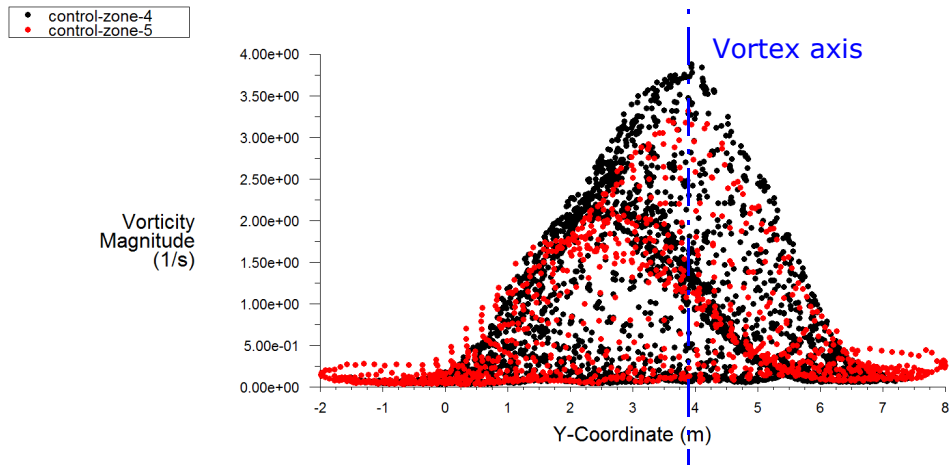
**Graphic.2: vorticity magnitude vs. Y-coordinate. Wingtip surface (transform-30). Blended winglet at 4°.**



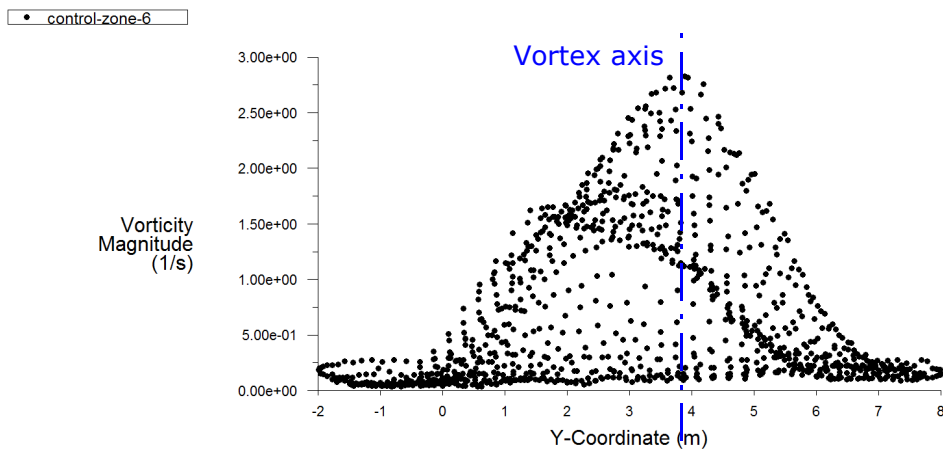
**Graphic.3: vorticity magnitude vs. Y-coordinate. Control zone-1. Blended winglet at 4°.**



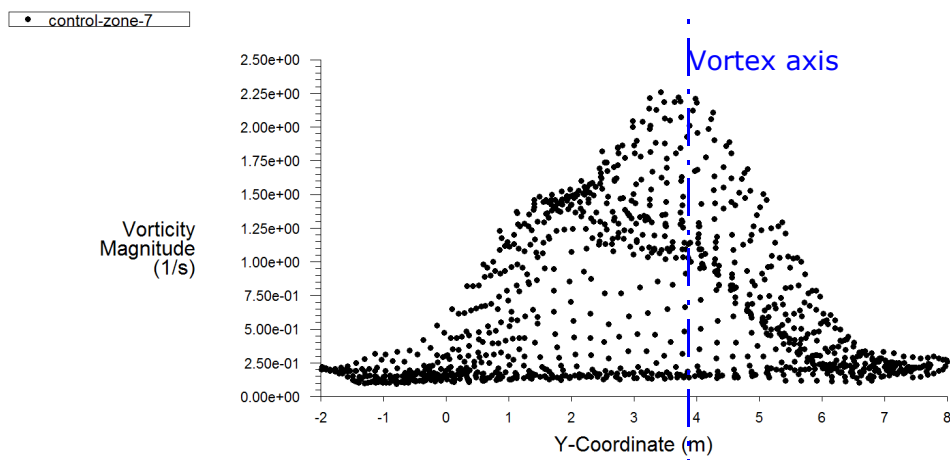
**Graphic.4: vorticity magnitude vs. Y-coordinate. Control zones-2 and 3. Blended winglet at 4°.**



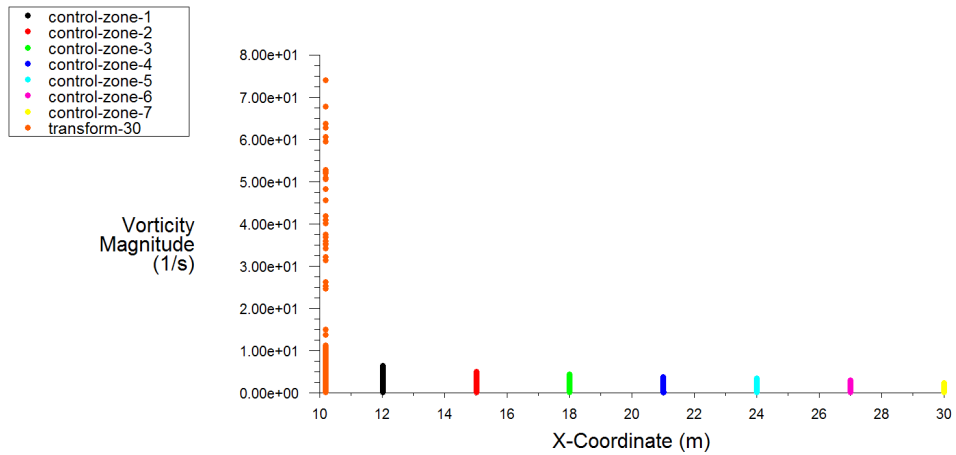
**Graphic.5: vorticity magnitude vs. Y-coordinate. Control zones-4 and 5. Blended winglet at 4°.**



**Graphic.6: vorticity magnitude vs. Y-coordinate. Control zone-6. Blended winglet at 4°.**

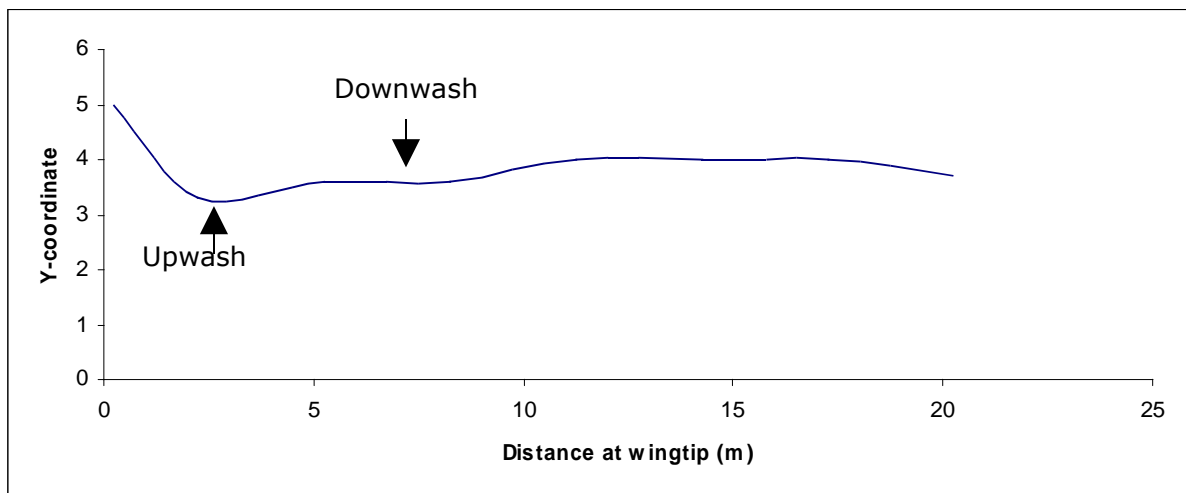


**Graphic.7: vorticity magnitude vs. Y-coordinate. Control zone-7. Blended winglet at 4°.**



**Graphic.8: vorticity magnitude vs. X-coordinate. All zones. Blended winglet at 4°.**

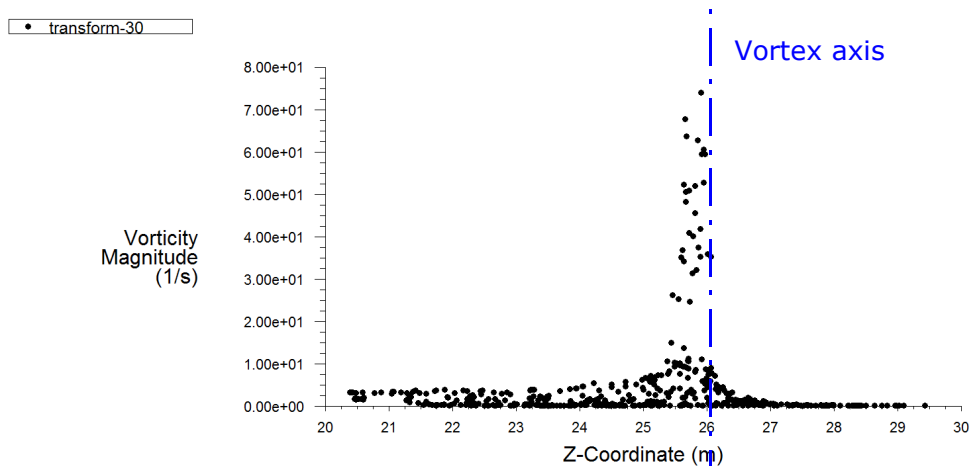
Like 0.25 m at the wingtip, graphic 2, vortex axis is placed at 5 m in Y-coordinate. About 2.25 m at the wingtip, vortex is placed at 3.3 m in Y-coordinate, graphic 3. In the control zones 2 and 3 vortex axis is placed at 3.5 m, graphic 4. In the control zones 4, 5 and 6, vortex axis is placed at 4 m at wingtip. Finally, about 20.25 m at the wingtip, control zone 7 and graphic 7, vortex axis is placed at 3.7 m in Y-coordinate. The next graphic will show the wingtip vortex axis motion and therefore, the wingtip vortex motion in grid Y-coordinate.



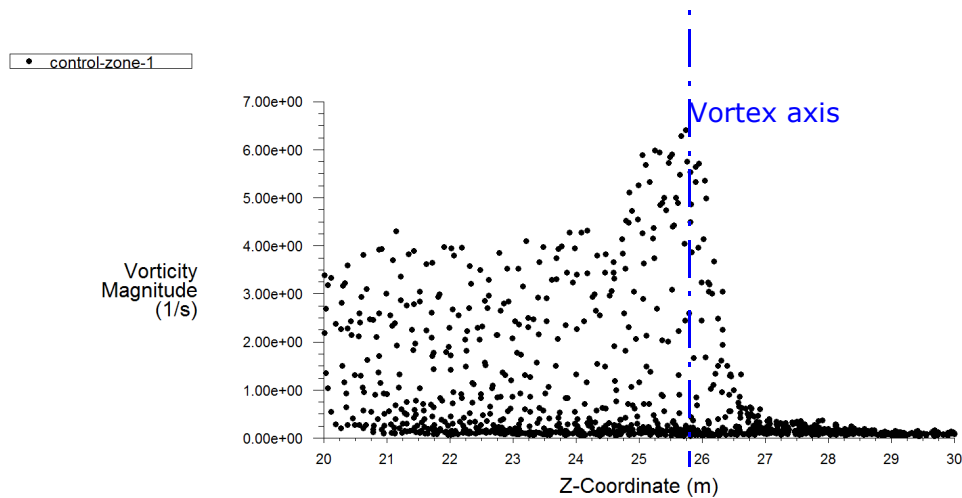
**Graphic.9: Y-coordinate vs. Distance at wingtip.**

Basically, to study how vortex moves laterally the procedure is very similar. However, we must use the perpendicular sheet plane and so, grid Z-coordinate will be used. To study how vortices move down and up, grid Y-coordinate has been used. To start out vortex motion laterally, I am going to show different graphs in the same zones that to study vortex motion down and up.

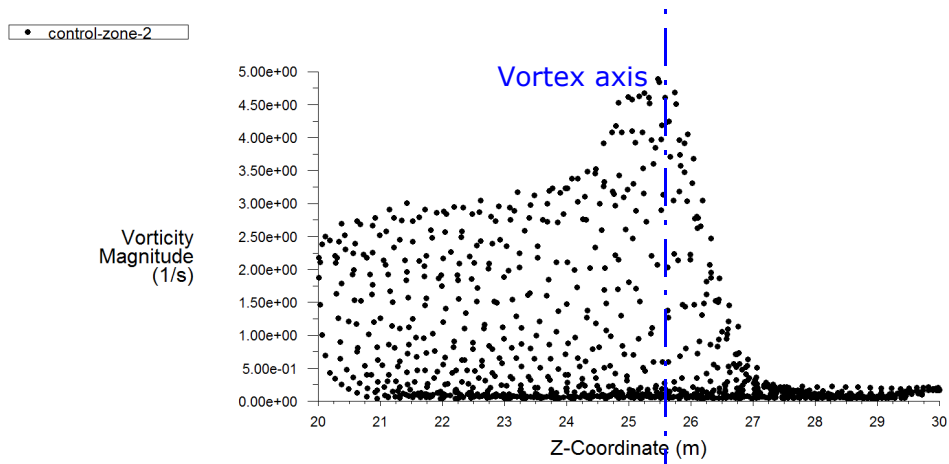
The following graphics show vorticity magnitude (1/s) versus grid Z-coordinate in the control zones and wingtip surface. Besides, a graphic where we can see the control zones and wingtip surface has been shown, graphic 8.



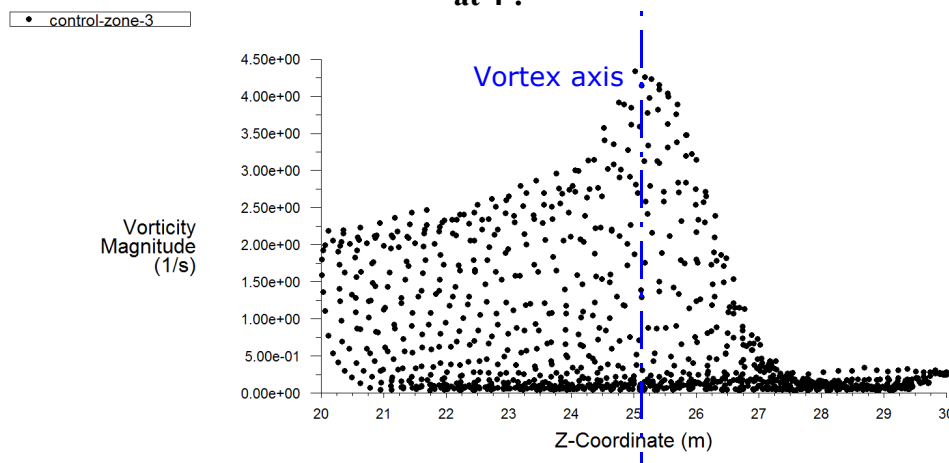
**Graphic.10: vorticity magnitude vs. Z-coordinate. Wingtip surface (transform-30). Blended winglet at 4°.**



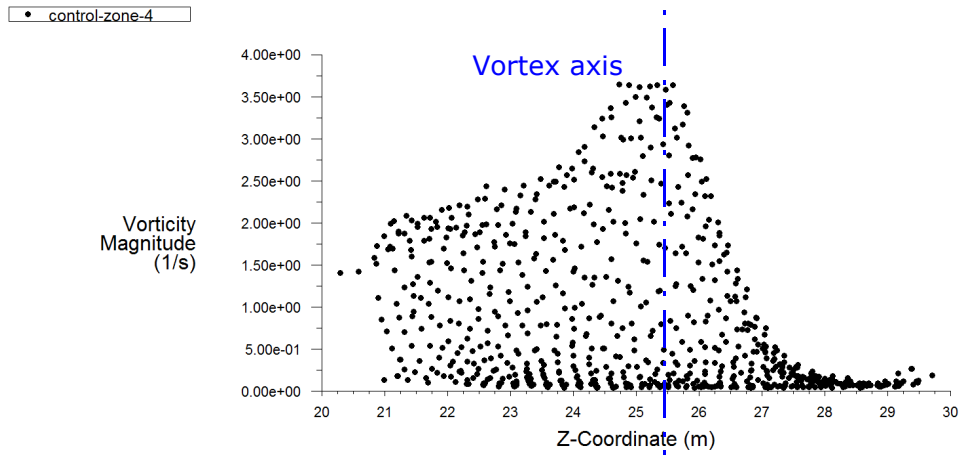
**Graphic.11: vorticity magnitude vs. Z-coordinate. Control zone-1. Blended winglet at 4°.**



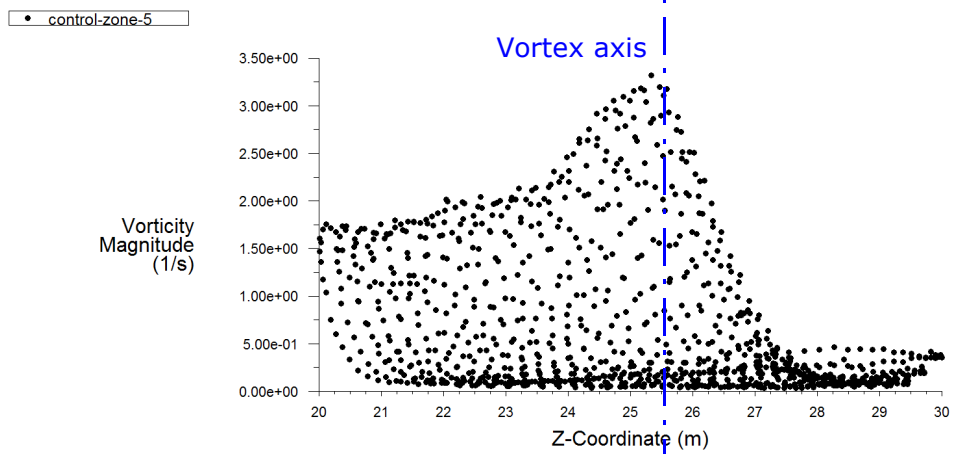
**Graphic.12: vorticity magnitude vs. Z-coordinate. Control zone-2. Blended winglet at 4°.**



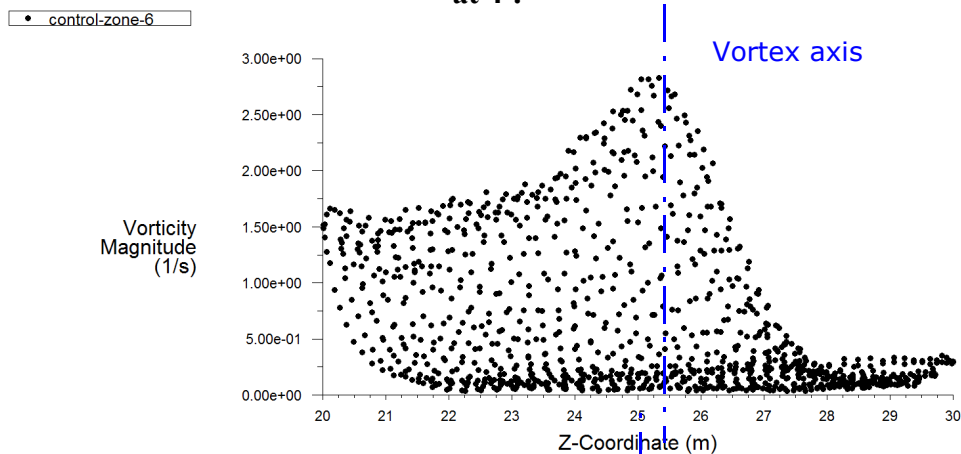
**Graphic.13: vorticity magnitude vs. Z-coordinate. Control zone-3. Blended winglet at 4°.**



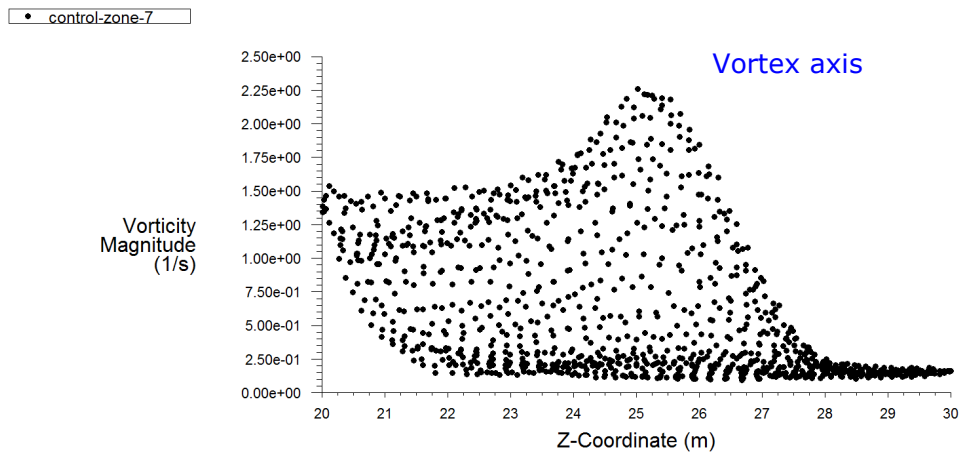
**Graphic.14: vorticity magnitude vs. Z-coordinate. Control zone-4. Blended winglet at 4°.**



**Graphic.15: vorticity magnitude vs. Z-coordinate. Control zone-5. Blended winglet at 4°.**



**Graphic.16: vorticity magnitude vs. Z-coordinate. Control zone-6. Blended winglet at 4°.**



**Graphic.17: vorticity magnitude vs. Z-coordinate. Control zone-7. Blended winglet at 4°.**

As can be seen from graphics 10 until 17, the wingtip vortex is between 26 m and 25 m grid Z-coordinate. At the beginning, the vortex axis is close to 26 m, wingtip surface and control zones 1 and 2. Besides, as vortex begins at 26 m in Z-coordinate (graphic 10), the wing length in Z-coordinate is 26 m. From control zone 2, the vortex axis begins to get away from the reader about 1 m in the perpendicular sheet plane. If grid Z-coordinate has a value higher means it is more close to reader. On the other hand, if the grid Z-coordinate value decreases the wingtip vortex gets away from the reader. Therefore, the vortex axis gets away from the reader when it moves away from wingtip. Until now, when and why wingtip vortices are created, vortex rotation and vortex motion have been explained. From now, winglet performance will be discussed.

### 5.3 Winglets performance

Aircrafts of all types and sizes are flying with winglets. When winglets are linked to wingtips, aircraft designers are looking for drag coefficient reduction and therefore, fuel consumption decreases. The wingtip vortices are responsible for the appearance of a drag coefficient component, induced drag coefficient  $C_{di}$ . In this section, I am going to try to demonstrate how wingtips vortices are reduced when winglets are used. In order to do that, control zones will be used to measure the vorticity magnitude in my four wing models. The models will be analysed in different angles of attack, between 4 and 12 degrees.

#### **5.3.1 Winglets performance at 4°**



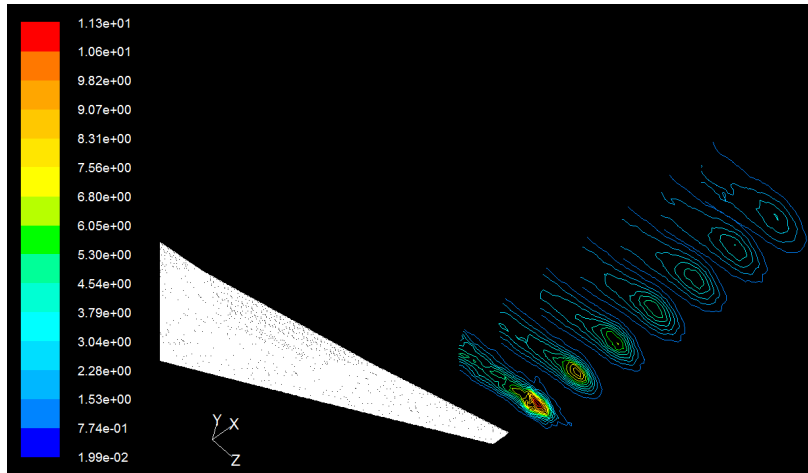


Fig.47: contours of vorticity magnitude 4°. No winglet. Orthographic projection.

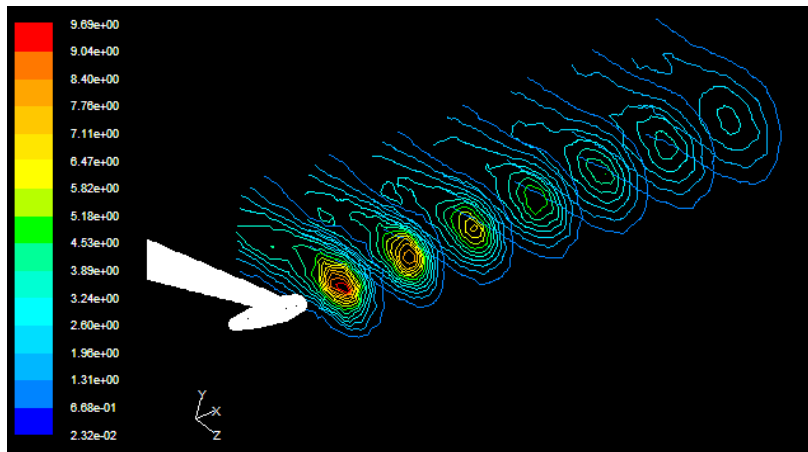


Fig.48: contours of vorticity magnitude 4°. Circular winglet. Orthographic projection.

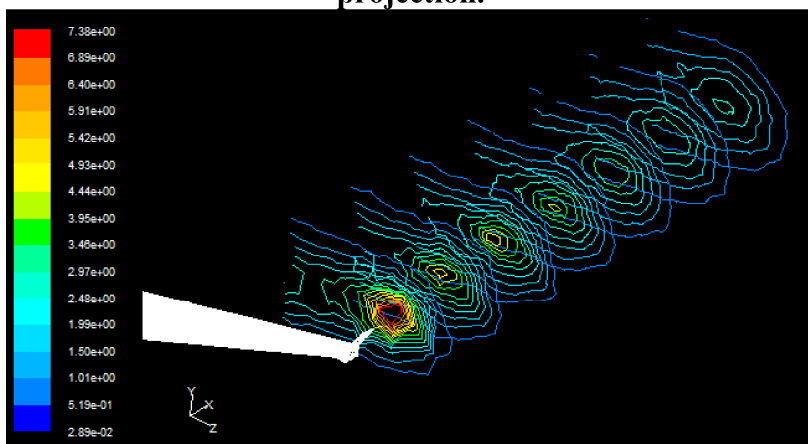
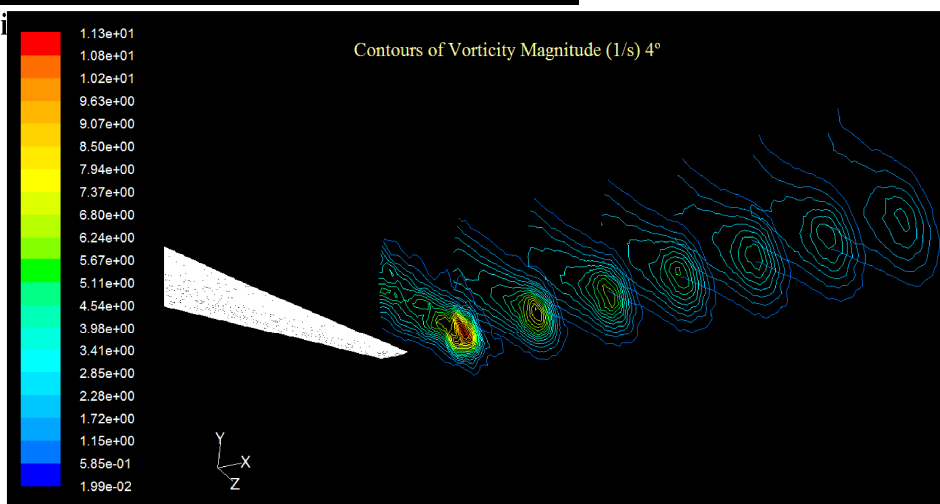
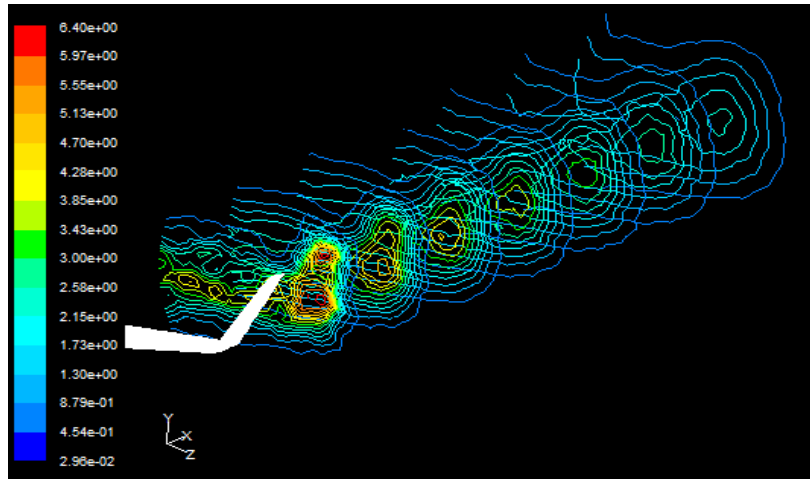


Fig.49: contours of vorticity





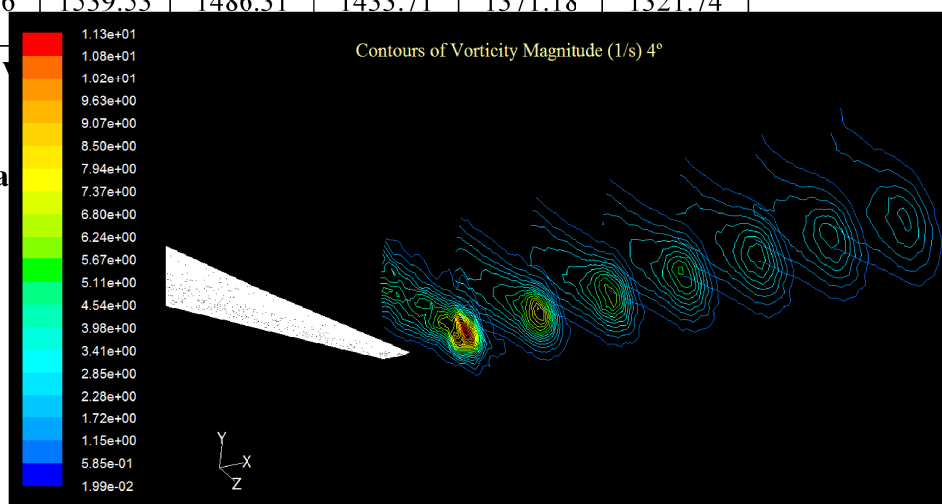
**Fig.50: contours of vorticity magnitude 4°. Blended winglets. Orthographic projection.**

The images, reproduced above, show the maximum value of vorticity magnitude decreases when winglets are fixed to wingtips. The maximum value of vorticity magnitude at 4 degrees in control zones occurs in wing model without winglet and it equals 11.3 (1/s). Circular winglet has a value of 9.69 (1/s). The smallest value occurs with blended winglet and it is 6.4 (1/s). It is absolutely important to measure vorticity magnitude, the control zones are the same distance from wingtip. The control zones must be located at the same distance from wingtip in grid X-coordinate. The table 2, reproduced below, shows the values of total sum of vorticity magnitude in control zones. The maximum total sum of vorticity magnitude value is produced by wing model without winglet and, the minimum value by wingtip fence. However, the minimum value of vorticity magnitude occurs with blended winglet.

<b>Wing model</b>	Zone-1	Zone-2	Zone-3	Zone-4	Zone-5	Zone-6	Zone-7
<b>Without winglet</b>	2012.3	1744.13	1646.84	1594.25	1543.52	1488.56	1434.83
<b>Circular winglet</b>	1827.1	1596.89	1524.99	1368.36	1310.32	1248.38	1205.94
<b>Wingtip fence</b>	1576.5	1455.18	1423.3	1386.76	1335.6	1272.44	1194.78
<b>Blended winglet</b>	1786.1	1593.06	1539.53	1486.31	1433.71	1371.18	1321.74

**Table.2: total sum of**

### 5.3.2 Winglets performance a



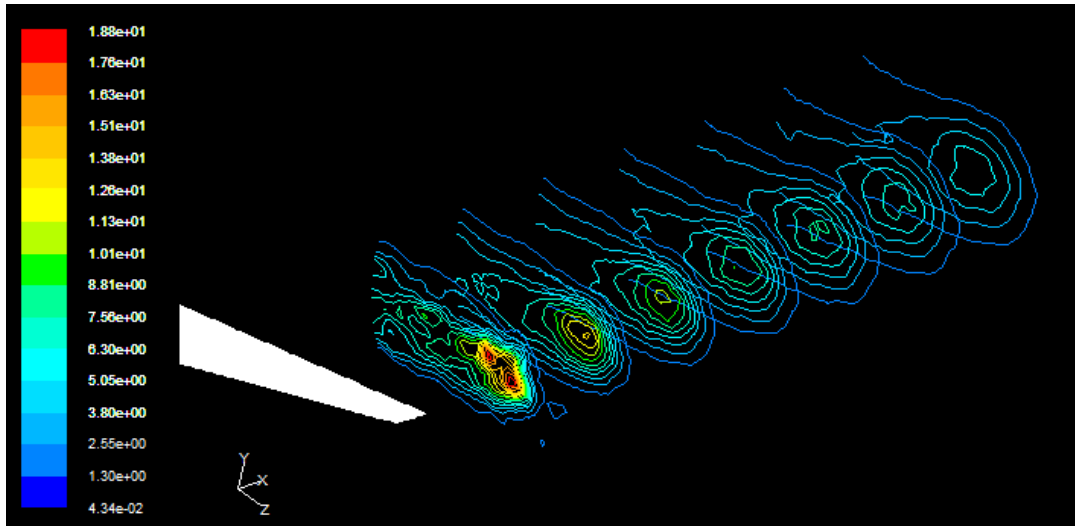


**Fig.51: contours of vorticity magnitude  $8^\circ$ . No winglet. Orthographic projection.**

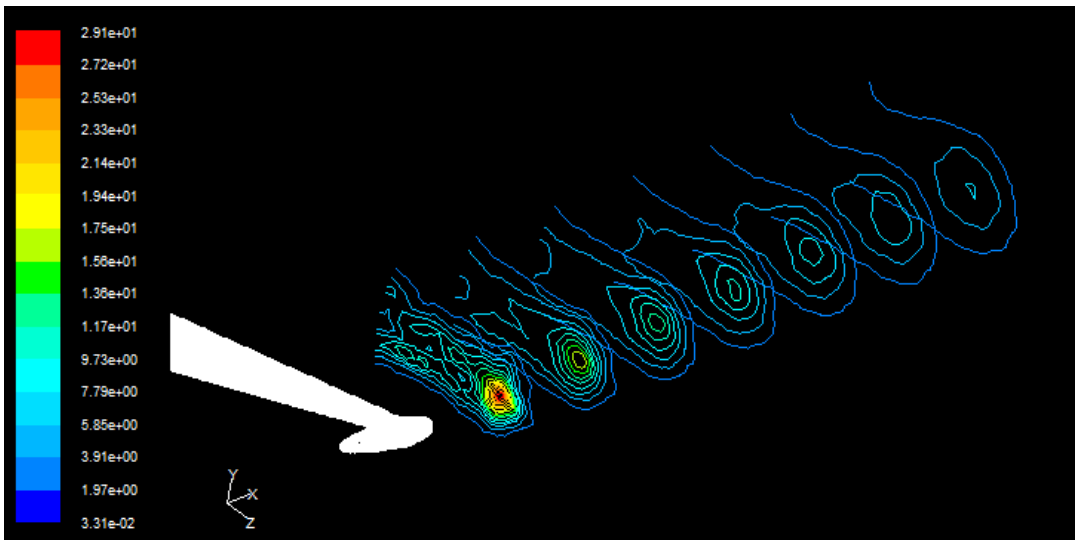


**Fig.52: contours of vorticity magnitude  $8^\circ$ . Circular winglet. Orthographic projection.**

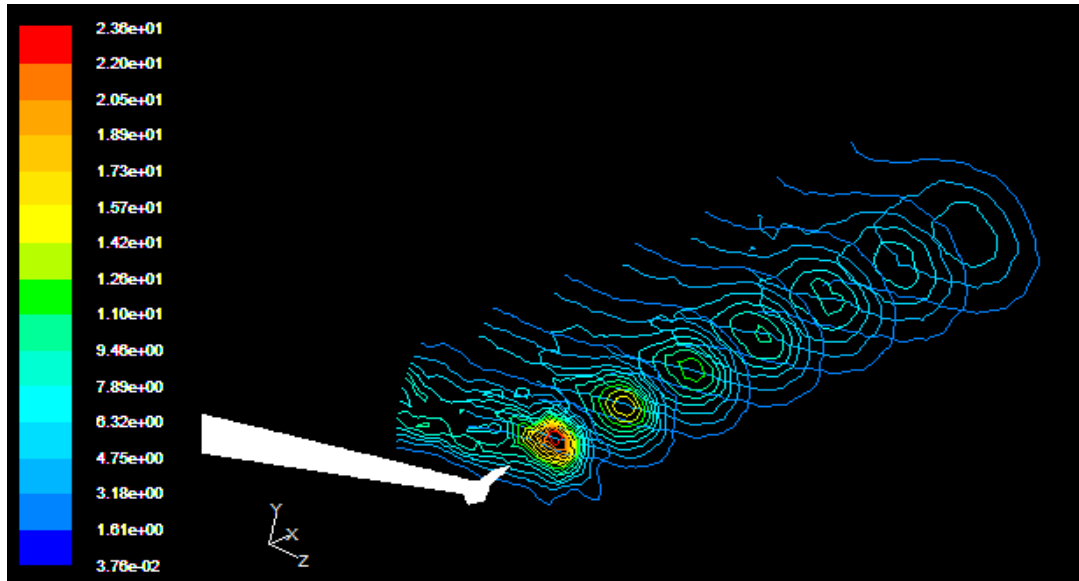


**Fig.53: contours of vorticity magnitude 8°. Wingtip fence. Orthographic projection.**

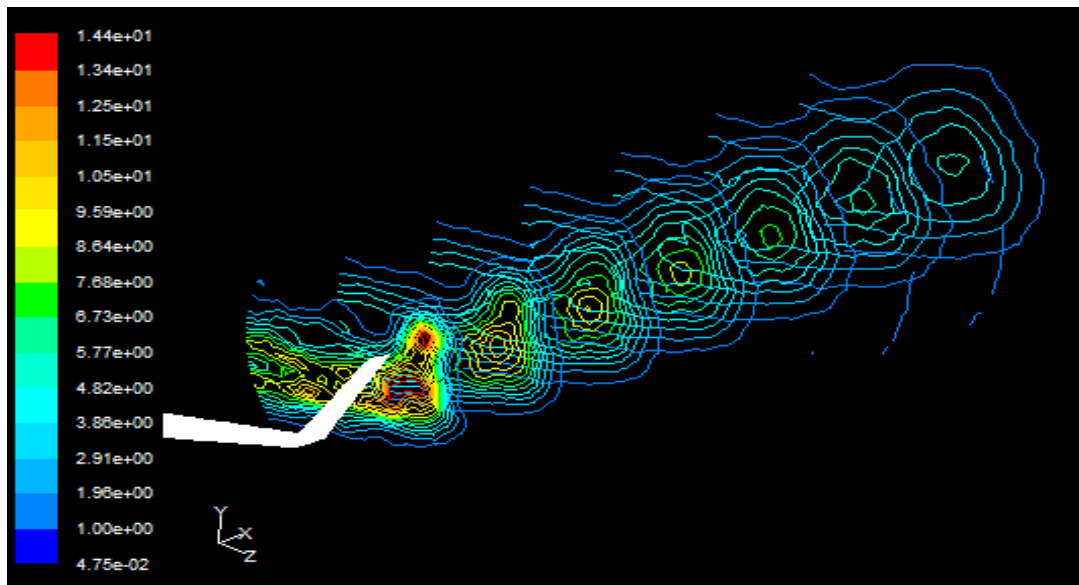


**Fig.54: contours of vorticity magnitude 8°. Blended winglet. Orthographic projection.**

<b>Wing model</b>	Zone-1	Zone-2	Zone-3	Zone-4	Zone-5	Zone-6	Zone-7
<b>Without winglet</b>	3668.25	3223.89	3109.14	2917.71	2925.78	2812.71	2669.59
<b>Circular winglet</b>	3536.26	2993.61	2827.98	2721.55	2628.22	2510.58	2400.33
<b>Wingtip fence</b>	3297.4	2821.4	2697.23	2620.41	2548.32	2446.13	2353.61
<b>Blended winglet</b>	3032.51	2663.86	2556.79	2511.77	2433.79	2329.23	2148.17

Table.3: total sum of vorticity magnitude (1/s) at 8° in control zones.

### 5.3.3 Winglets performance at 12°

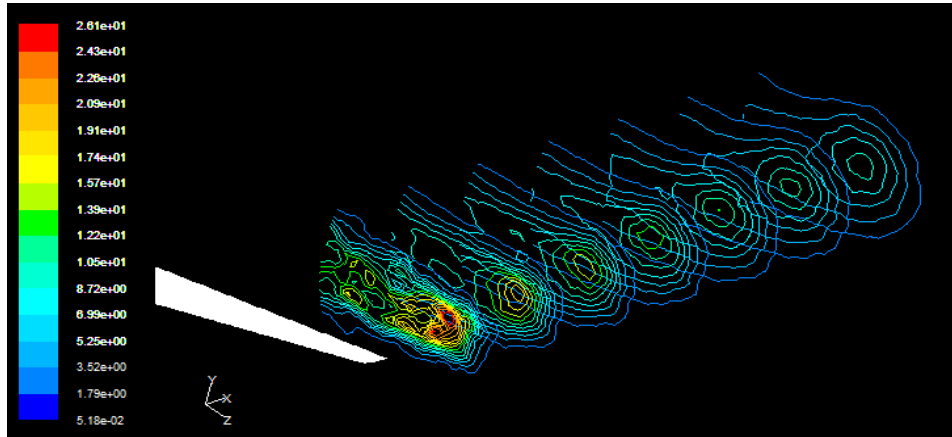


Fig. 55: contours of vorticity magnitude 12°. No winglet. Orthographic projection.

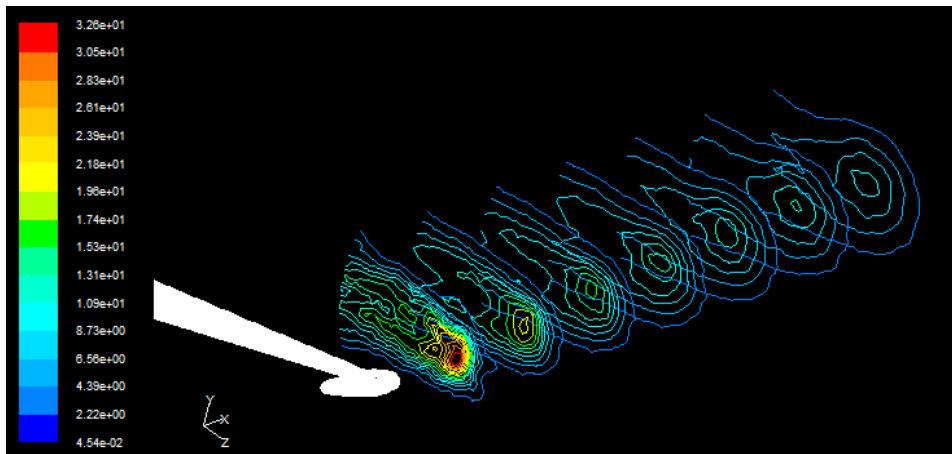
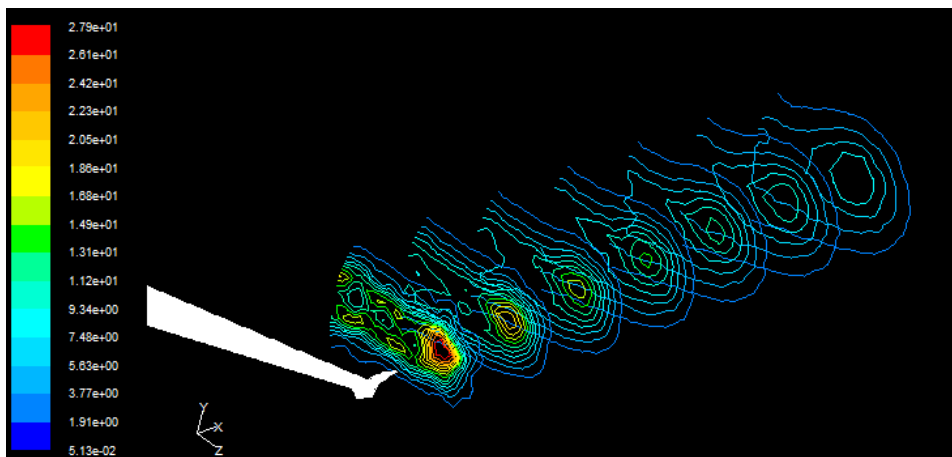
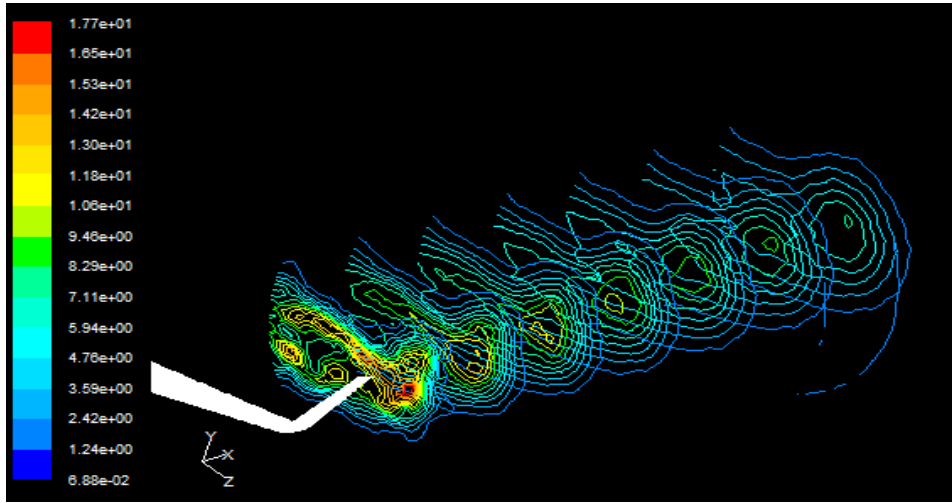


Fig.56: contours of vorticity magnitude 12°. Circular winglet. Orthographic projection.



**Fig.57: contours of vorticity magnitude 12°. Wingtip fence. Orthographic projection.**



**Fig.58: contours of vorticity magnitude 8°. Blended winglet. Orthographic projection.**

<b>Wing model</b>	Zone-1	Zone-2	Zone-3	Zone-4	Zone-5	Zone-6	Zone-7
<b>Without winglet</b>	6133.68	5185.92	4890.39	4710.73	4553.77	4381.43	4171.45
<b>Circular winglet</b>	5900.48	4893.3	4530.3	4297.28	4105.32	3904.47	3718.92
<b>Wingtip fence</b>	5430.57	4692.14	4498.31	4361.97	4237.1	4075.23	3854.51
<b>Blended winglet</b>	5307.19	4410.26	4158.24	4007.91	3878.88	3734.62	3578.11

**Table.4: total sum of vorticity magnitude (1/s) at 12° in control zones.**

As can be seen from tables 2 until 4, the minimum total sum of vorticity magnitude value is produced in wing models with wingtip fence or blended winglet. The maximum value of total sum of vorticity magnitude is always produced in wing model without winglet. Furthermore, the second maximum value of total sum of vorticity magnitude is always produced by wing model with circular winglet. With an angle of attack of 4 degrees, wingtip fence is able to get the highest wingtip vortex reduction in control zones. Nevertheless, blended winglet works better at 8 and 12 degrees. Blended winglet works better at 16° again, table not reproduced. To measure sum of vorticity magnitude, we must use *report* → *surface integrals* option into Fluent. Once there, *report type* → *sum*, *field variable* → *velocity* → *vorticity magnitude* and finally, *surfaces* → *control zones*. It is clear; winglets are able to reduced wingtip vortex vorticity magnitude. If

wingtip vortex is reduced, the induced drag associated with wingtip vortices development goes down and therefore, drag decreases and aircraft's performance is improved. We can check drag coefficient improvement in section 5.5. In the next section, an attempt to explain how winglets reduced wingtip vortex will be made.

#### 5.4 Wingtip vortex reduction

In this section, I would like to discuss about winglets can reduced wingtips vortex. In the previous section, we saw winglets reduce wingtip vortices (George Larson, 2001), the twin tornados formed by the difference between the pressure on the upper surface of an airplane's wing and that on the lower surface. High pressure on the lower surface creates a natural airflow that makes its way to the wingtip and curls upward around it. When flow around the wingtips streams out behind the airplane, a vortex is formed. These twisters represent an energy loss and are strong enough to flip airplanes that blunder into them.

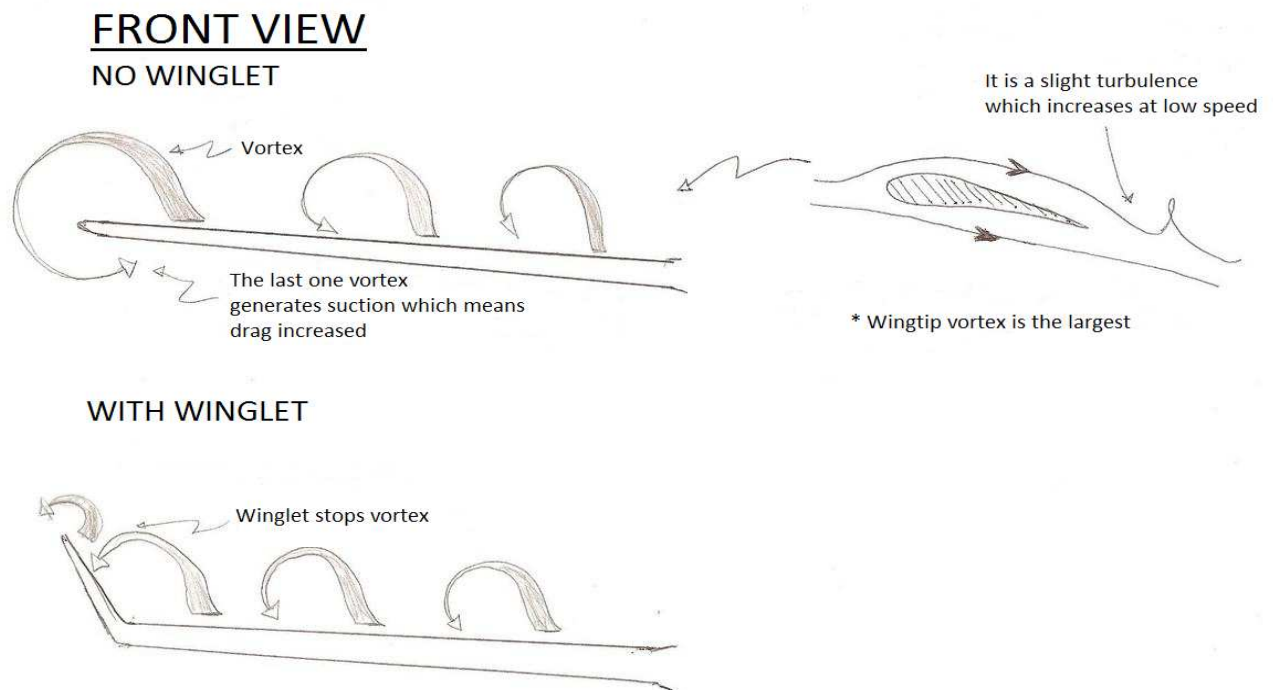


**Fig. 59: wingtip vortex reduction.**

At the wing front, along the upper surface of the wing are small vortices along the wing surface, that as a result of right wing and gets higher as you reach the end of the wing.

When you get there, this vortex generates suction, which in turn creates resistance. The function of the winglet is to reduce the size of the vortex. Thus, it is strongly suitable to link a barrier (winglet) at wingtips. That is the concept of winglets. Winglet attracted to him the vortex and the vortex is deflected far over the wing. To finish this section, I am going to talk about aerodynamic forces lift and drag and their coefficients.

### 5.5 Drag coefficient improvement

The main aim of my project is to check how winglets are able to reduced drag coefficient. The following tables show wing models drag coefficient is reduced when winglets are linked to wingtips with different angles of attack, between 4° and 16°.

Angle of Attack	Lift (KN)	Drag (KN)	$C_d$	$CL$	$CL/C_d$
4°	191.31111	17.4328	0.014612	0.160368	10.9745
8°	373.99611	36.0350	0.030215	0.313499	10.3807
12°	523.08733	67.2566	0.056377	0.438477	7.77742
16°	633.51104	113.1905	0.094881	0.531038	5.59968

**Table.5: aerodynamic coefficients. Without winglet.**

Angle of Attack	Lift (KN)	Drag (KN)	$C_d$	$CL$	$CL/C_d$
4°	193.70024	17.9516	0.014727	0.158912	10.7901
8°	374.85585	36.9668	0.030380	0.308125	10.1429
12°	527.00923	69.6431	0.057239	0.433225	7.56861
16°	634.46797	118.0409	0.097027	0.521512	5.37489

**Table.6: aerodynamic coefficients. Circular winglet.**

Angle of Attack	Lift (KN)	Drag (KN)	$C_d$	$CL$	$CL/C_d$
4°	191.9359	17.4708	0.014578	0.160070	10.9802
8°	373.5895	36.3083	0.030299	0.311754	10.2892
12°	524.6641	67.8154	0.056512	0.437215	7.73667
16°	636.0733	115.8315	0.096661	0.530792	5.49133

**Table.7: aerodynamic coefficients. Wingtip fence.**

Angle of Attack	Lift (KN)	Drag (KN)	$C_d$	$CL$	$CL/C_d$
4°	192.7925	17.6652	0.014625	0.159613	10.9136
8°	370.9876	36.0023	0.029759	0.307142	10.3209
12°	524.2974	67.2123	0.055641	0.434069	7.80122
16°	635.7335	113.5871	0.094039	0.526329	5.59682

**Table.8: aerodynamic coefficients. Blended winglet.**



In the tables reproduced above, we can see drag coefficient decreases with wing model wingtip fence and blended winglet. That drag coefficient decrease is measured respect to wing model without winglet. At 4°, the smallest drag coefficient is equal to 0.014578, wingtip fence. At 8°, it is equal to 0.029759, blended winglet. At 12°, it equals 0.0434069, blended winglet. Finally, it is equal to 0.094039 at 16° in blended winglet. Also, we can see circular winglet drag coefficient is higher than wing model no winglet drag coefficient. Circular winglet is able to reduce vorticity magnitude behind wingtips. Therefore, it is able to reduce induced drag coefficient,  $C_{di}$ . However, induced drag coefficient is one of drag coefficient components. The wing model with circular winglet reference area is larger than without winglet (table1) and that is why circular winglet  $C_d$  is higher. Thus, the circular winglet shape is not very correct and appropriate. It is not very difficult to reduce wingtip vortex (circular winglet) although to get  $C_d$  reduction is much complex.

Angle of Attack	$C_d$ NO WINGLET	$C_d$ BEST WINGLET	WINGLET	IMPROVEMENT
4°	0.014612	0.014578	WINGTIP FENCE	0.232 %
8°	0.030215	0.029759	BLENDED WINGLET	1.509 %
12°	0.056377	0.055641	BLENDED WINGLET	1.305 %
16°	0.094881	0.094039	BLENDED WINGLET	0.887 %

**Table.9: drag coefficient improvement.**

The table 9 shows the best  $C_d$  improvement occurs at 8° with blended winglet. The wingtips vortices intensity is related to lift. If the wing is working with high angles of attack the lift is increased. Therefore, we can expect winglet works better with large angles of attach, since the wingtip vortex reduction will be higher. Wingtip fence works better with low angles of attack and blended winglet works better with high angles of attack. The best winglet is blended winglet because of it is able to reduced  $C_d$  conveniently, and the best drag coefficient reduction occurs when it is working.

## 6 CONCLUSIONS

The wingtip vortex are developed as a wing is able to produce a ratio  $Cl/Cd$  higher than 1. If ratio  $Cl/Cd$  is less than 1, there are no wingtip vortices since the wing is not operating a positive lift. To produce a ratio  $Cl/Cd$  higher than 1, the pressure of the lower surface must be higher than the pressure of the upper surface, as can be seen from figures 35 until 38. The difference pressure between lower and upper surface in a wing generates lift and therefore wingtip vortices. The vorticity magnitude increases respect to angle of attack due to the lift increases as the angle of attack goes up.

My wings models are placed on the right of the aircraft, so the vortex rotation moves anticlockwise from a front view. Lower surface is the zone where the pressure takes its highest value, and also in the upper surface the value of pressure is smaller than lower surface, figure 34 until figure 38. The air goes up from the lower and upper surface and then, the wingtips vortices spin anticlockwise, figure 40 and graphic 1. The vortex axis starts out at the same height as the wingtip or winglet tip, figure 44 and its axis moves down and up, graphics 2 until 9. Furthermore, the vortex axis moves away sideways from the wingtip, graphics 10 until 17. The maximum value is placed into the wingtip vortex axis and wingtip vortex is turning around on its own axis. Also, vortex widens as it moves away from the wingtip. The vortex lost intensity as we move away from the wingtip, tables 2, 3 and 4.

The function of the winglet is to reduce the size of the vortex. Winglet attracted to him the vortex and the vortex is deflected far over the wing. The three wing models with winglet are able to reduce the vorticity magnitude in control zones, tables 2 until 4.

Therefore, the induced drag  $Cdi$  goes down in all my wing models with winglet.

However, wing model with circular winglet is not able to reduce drag coefficient  $Cd$ .

Circular winglet design was not suitable and acceptable. It is not very difficult to reduce wingtip vortex (circular winglet) although to get  $Cd$  reduction is much complex. On the other hand, wingtip fence and blended winglet are able to reduce wing model without winglet drag coefficient. Wingtip fence model works at 4 degrees correctly, table 9. The vorticity magnitude is not very large at 4 degrees, so wingtip fence model works better at low angles of attack. The best winglet is blended winglet model since, it is able to reduce drag coefficient as vorticity magnitude is higher. With an angle of attack of 8

degrees, the drag coefficient reduction is 1.509 %, table 9. I can affirm blended winglet and wingtip fence are tools that improve aircraft's performance when the aircraft is taking off.

## **7 RECOMMENDATIONS**

Blended winglet model and wingtip fence model should be made of different airfoil and then, drag coefficient reduction could be compared. Furthermore, circular winglet model should be re-designed due to its design's fail.

On the other hand, it would be highly interesting to end up by doing my computational fluids dynamics analysis when the aircraft is flying at cruise velocity.

## 8 REFERENCES

Aerotecología, 2010. *¿Qué es un winglet?*. [online] Available at :< <http://aerotecologia.blogspot.com/2010/09/que-es-un-winglet.html>> [Accessed 25 January 2010].

Airline world. *Aircraft Winglets*. [online] Available at :< <http://airlineworld.wordpress.com/2008/10/01/aircraft-winglets/>> [Accessed 25 November 2010].

Aviation Partners Boeing, 2006. *Winglets*. [online] Available at :< <http://www.aviationpartnersboeing.com/winglets/index.html>> [Accessed 12 November 2010].

Ardua ad Astra, 2006. *Vórtices, winglets y demás parafernalia aeronáutica*. [online] Available at :< <http://perarduaadastra.eu/2010/10/vortices-winglets-y-demas-parafernalia-aerodinamica/>> [Accessed 22 October 2010].

Boeing, 2009. *Advanced Blended Winglets*. [online] Available at :< <http://www.b737.org.uk/winglets.htm#Newsstories>> [Accessed 12 January 2011].

Eduardo Nuñez, 2010. *Winglets*. [online] Available at :< [http://www.nurflugel.es/index.php?option=com\\_content&view=article&id=109%3Awinglets&catid=9%3Adise&Itemid=12](http://www.nurflugel.es/index.php?option=com_content&view=article&id=109%3Awinglets&catid=9%3Adise&Itemid=12)> [Accessed 20 October 2010].

Enciclopedia de Física. *Resistencia aerodinámica*. [online] Available at :< <http://www.esacademic.com/dic.nsf/eswiki/278508>> [Accessed 25 January 2010].

George Larson, 2001. *How Things Work: Winglets*. [online] Available at :< <http://www.airspacemag.com/flight-today/wing.html>> [Accessed 1 December 2010].

Marty Curry, 2008. *Winglets*. [online] Available at :< <http://www.nasa.gov/centers/dryden/about/Organizations/Technology/Facts/TF-2004-15-DFRC.html> > [Accessed 1 November 2010].

M.A.Soliman, 2009. *Viscosity measurement*. [online] Available at :< <http://dr mohamedsoliman.blogspot.com/2009/09/viscosity-measurement.html> > [Accessed 25 November 2010].

NASA. *Induced Drag Coefficient*. [online] Available at :< <http://www.grc.nasa.gov/WWW/K-12/airplane/induced.html> > [Accessed 25 January 2010].

Robert Faye, Robert Lapetre, Michael Winter. *Aero 17*. [online] Available at :< [http://www.boeing.com/commercial/aeromagazine/aero\\_17/winglet\\_story.html#bbj](http://www.boeing.com/commercial/aeromagazine/aero_17/winglet_story.html#bbj)> [Accessed 25 October 2010].

Tipler, Paul; Mosca, Gene. 2010, *Física para la ciencia y tecnología*. 6th ed. Editorial Reverté S.A.

Tom Bensom, 2010. *Four forces on an airplane*. [online] Available at :< <http://www.grc.nasa.gov/WWW/K-12/airplane/forces.html> > [Accessed 1 April 2010].

Tom Bensom, 2009. *The lift coefficient*. [online] Available at :< <http://www.grc.nasa.gov/WWW/K-12/airplane/liftco.html> > [Accessed 1 April 2010].

Tom Bensom, 2010. *The drag coefficient*. [online] Available at :< <http://www.grc.nasa.gov/WWW/K-12/airplane/induced.html> > [Accessed 1 April 2010].

U.S. Centennial of Flight Commission. Wing Vortices. [online] Available at :<  
[http://www.centennialofflight.gov/essay/Theories\\_of\\_Flight/Vortex/TH15.htm](http://www.centennialofflight.gov/essay/Theories_of_Flight/Vortex/TH15.htm)>  
[Accessed 18 February 2010].

## 9 APPENDIX A

An attempt was made to analyse the different wing models when the aircraft works in cruise velocity. Unfortunately, as I was running out of time, this task was not successfully completed. However, I would like to explain the steps to solve the problem in Fluent.

### Cruise velocity in Fluent

1. *File* → *Read* → *Case*. Navigate to the working directory and select the .msh file.
2. *Grid* → *Check*. Any errors in the grid would be reported at this time.
3. *Grid* → *Info* → *Size*.
4. *Grid* → *Scale*. We must define grid units.

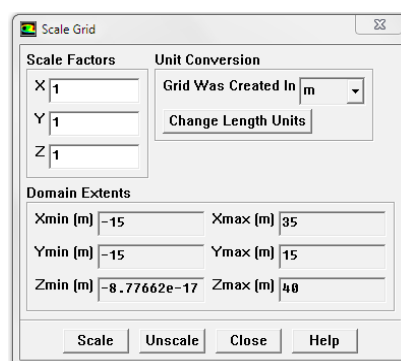


**Fig.60: grid scale. Cruise velocity.**

5. *Grid* → *Display*. We can look at specific parts of the grid by choosing the boundaries you wish to view under Surfaces. The surface linked to the wing and the wing are walls, in black. The rest of the surfaces are pressure farfield, in pink. Control zones, in green.

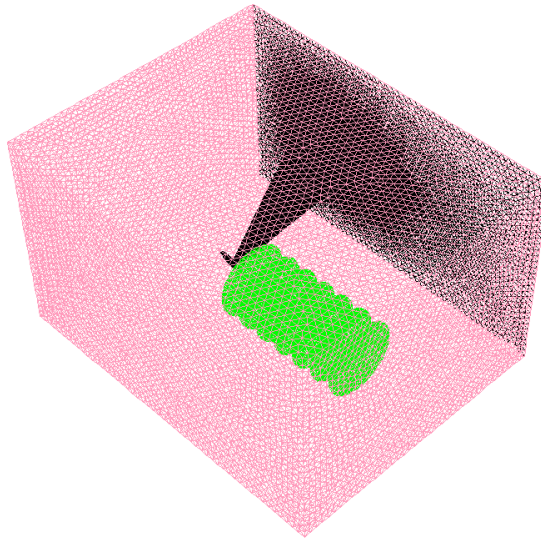


**Fig.61: isometric view grid. Cruise velocity.**

6. *Define* → *Models* → *Solver*. We tick Unsteady under Time, 2nd-Order Implicit under Unsteady Formulation and Green-Gauss Node Based under Gradient Options.

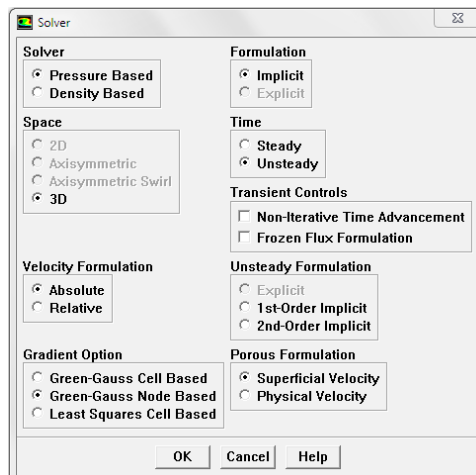


**Fig.62: Solver. Cruise velocity.**

7. *Define* → *Models* → *Energy*. We have to use Energy Equation since air flow will be compressible.

8. *Define* → *Models* → *Viscous*. We must use k- $\omega$  SST (Shear Stress Transport).

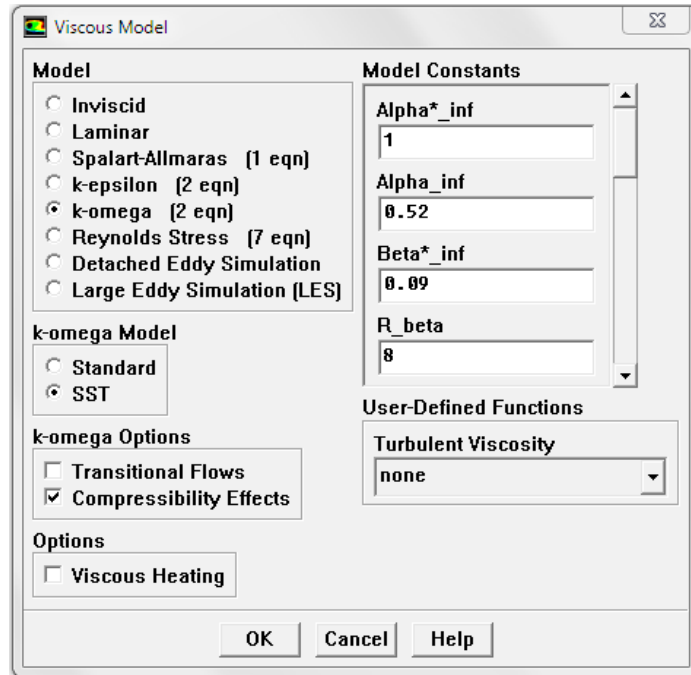


**Fig.63: viscous model. Cruise velocity.**

9. *Define* → *Materials*. Under Properties, we pick ideal-gas to take into account compressibility effects. We select sutherland into Viscosity.

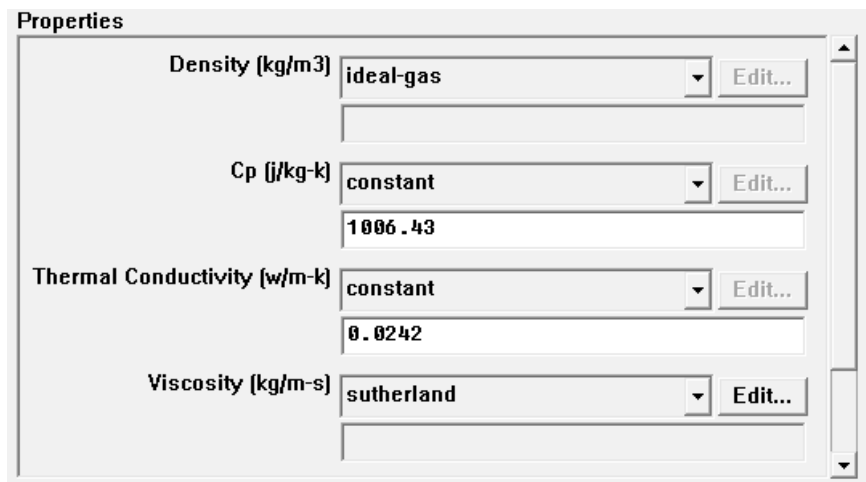


**Fig.64: materials. Cruise velocity.**

10. *Define* → *Operating Conditions*. Operating Pressure equals 0 Pa.

11. *Define* → *Boundary Conditions*. Under zone, we select farfield. In the volume control (wing tunnel), the surface link to the wing is wall. The rest of surfaces are pressure farfield. We set Mach Number equals 0.85 (254 m/s cruise velocity), Pressure



equals 22700 Pa and Temperature 223 K, according to International Standard Atmosphere (ISA).

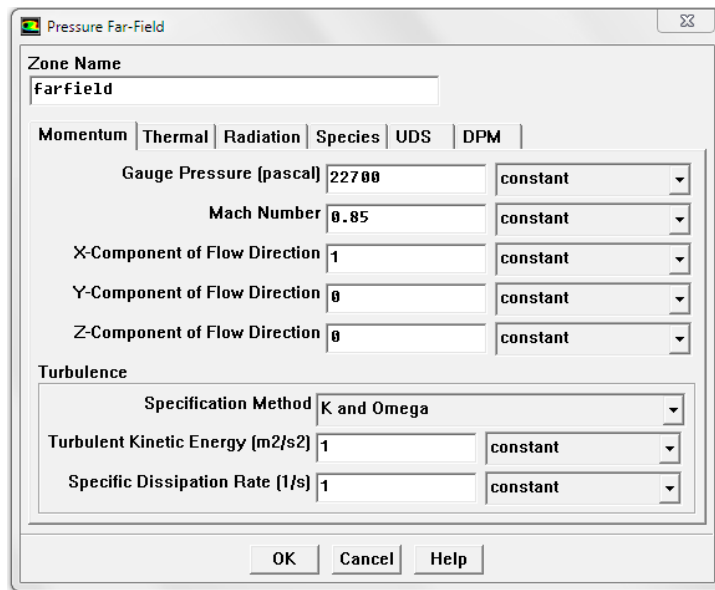


**Fig.65: boundary conditions. Cruise velocity.**

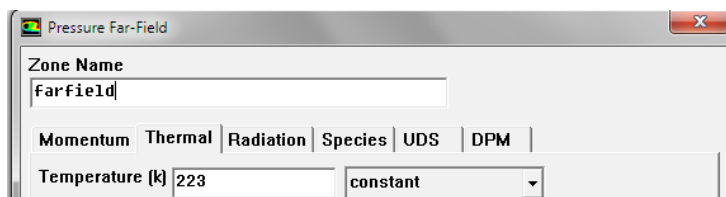


**Fig.66: boundary conditions. Cruise velocity.**

12. *Solve* → *Controls* → *Solution*. Under Pressure-Velocity Coupling, we must select Coupled option. Under Discretization, Second Order.

13. *Solve* → *Initialize* → *Initialize*. Compute From farfield and click Init.

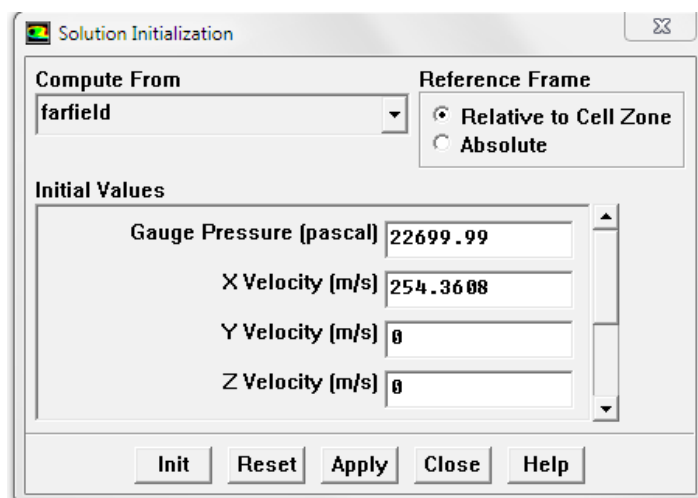


**Fig.67: Initialize. Cruise velocity.**

14. *Solve* → *Monitors* → *Residual*. Under Options, select Print and Plot.
15. *Solve* → *Monitors* → *Force*. Under Options, select Print and Plot. Under coefficient, select Drag (Force Vector [1,0,0]) and select Lift (Force Vector [0,1,0]). Finally, we select wing under Wall Zones.
16. *Report* → *Reference Values*. Compute From farfield and we must write Area and Length.
17. *Solve* → *Case Check*. Any errors in the previous steps will be reported at this time.
18. *File* → *Write* → *Case*.
19. *Solve* → *Iterate*. Time step size: it is the time that happens between consecutives calculus. Number of Time Steps: it is the amount of times that the software makes the same calculus, decreasing mistake made.
20. *File* → *Write* → *Case & Data*. To save the file.